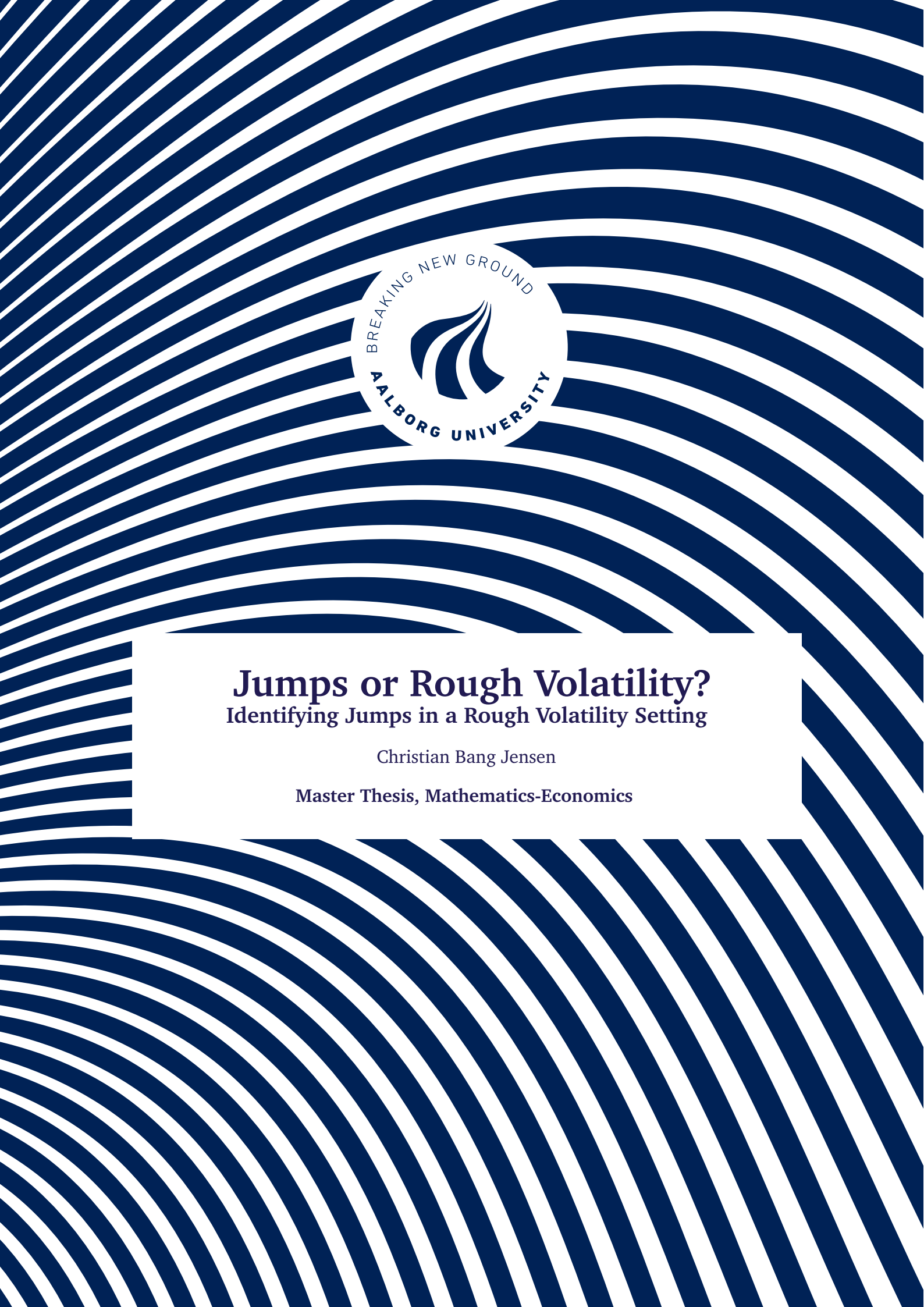

Jumps or Rough Volatility?

Identifying Jumps in a Rough Volatility Setting

Christian Bang Jensen

Master Thesis, Mathematics-Economics

Dept. of Mathematical Sciences
Skjernvej 4A
DK-9220 Aalborg Ø
http://math.aau.dk

AALBORG UNIVERSITY
STUDENT REPORT

Title
Jumps or Rough Volatility?

Theme
High-Frequency Econometrics

Project Period
Spring Semester 2024

Project Group
Group 4.111c_1

Participant
Christian Bang Jensen

Supervisor
Orimar Sauri

Page Numbers
62

Date of Completion
June 2, 2024

Abstract

High-frequency econometrics and testing for jumps in a high-frequency set-up are the main themes of this Master's thesis. We investigate how the ratio jump test introduced by Aït-Sahalia and Jacod performs, when it is tested on price processes, which contain a rough volatility component.

We start off by outlining some of the features that pertain to high-frequency data as well as how the realized covariation may be used to estimate the integrated volatility of the price process. Then we introduce the jump test, which utilizes a ratio of power variations at different frequencies to test for the presence of jumps.

After introducing stochastic delay differential equations (SDDE), we conduct a simulation study to investigate how the test performs in a rough set-up. For standard Itô semimartingales, the test performs largely as expected, which is also the case when we include jumps. We test two different rough models, where the first one models the log-volatility as a SDDE, and the second model is the rough fractional stochastic volatility model introduced by Gatheral et al. in [14].

Preface

This Master's thesis is written during the spring semester of 2024 as part of the Master's programme in Mathematics-Economics at the Department of Mathematical Sciences at Aalborg University.

The thesis is composed of numbered chapters with corresponding sections and subsections. Citations and external references are made using the Vancouver system such that [1, p. 10] refers to page 10 of the first entry in the bibliography. All programming is performed using R, and the code can be found at the following GitHub repository: `https://github.com/cbje18/MasterThesis`.

Finally, the author would like to extend his appreciation to his supervisor Orimar Sauri.

Signature

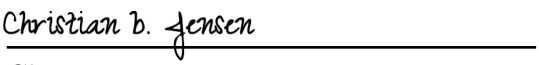

Christian Bang Jensen

Contents

1 Introduction

Volatility, a fundamental concept in financial mathematics, represents the degree of variation in the price of a financial instrument over time. It plays a critical role in risk management, derivative pricing, and portfolio optimization. Hence, the accurate modelling and forecasting of volatility is of paramount importance.

In the world of derivatives pricing, one often models the log-prices of some given asset S_t as a continuous semimartingale of the form

$$\mathrm{d}S_t = \mu_t \mathrm{d}t + \sigma_t \mathrm{d}B_t, \tag{1.1}$$

where μ_t is a suitable drift process, B_t is a one-dimensional standard Brownian motion, and σ_t is the volatility process. In the Black & Scholes model, the volatility is simply constant or a deterministic function of time. However, this is highly inconsistent with the actual implied volatilities observed in the markets, which has subsequently led to further development of models of the type in (1.1). As such, the classical stochastic volatility models were introduced, where the volatility component σ_t itself is some stochastic process. Furthermore, models that introduce jumps in the price process S_t have also found uses within quantitative finance. Jumps are especially pronounced in high-frequency financial data, which we elaborate on further in Chapter 2.

However, classical stochastic volatility models do not offer much flexibility in terms of the regularity of the volatility process. In a pioneering paper by Gatheral, Jaisson, and Rosenbaum [14], based on high-frequency data, they argue that volatility is characterized by less regular paths than assumed in classical models. They show that the log-volatility is well-characterized by a fractional Brownian motion of Hurst index $H < 1/2$. In [10], using a generalized method of moments approach, they estimate the Hurst index of the S&P 500 to be $H = 0.043$. This gives very erratic paths of the volatility process, which contains large spikes of volatility. Consequently, the paths of the price process behave more erratic and will have almost jump-like behaviour due to the spikes in volatility.

In this Master's thesis, we investigate whether tests developed to detect jumps in a discretely observed process can differentiate between actual jumps and rough volatility. In particular, we will investigate the test developed by Aït-Sahalia and Jacod in [1], which uses power variations at different frequencies to detect jumps in the process, and see how it fairs against processes driven by a rough volatility component.

1.1 Problem Statement

Based on the introduction above, the problem statement for the project can be stated as follows:

How does the Aït-Sahalia and Jacod jump test perform when tested on price processes driven by a rough volatility component, and it is able to distinguish between actual jumps and rough volatility?

2 High-Frequency Data Characteristics

In this chapter, we will investigate some of the properties that pertain to high-frequency financial data, which distinguish it from more conventional time series data. The chapter is based on [2, p. 57-77]

2.1 Mechanisms of Price Determination

The determination of the price of an asset traded in a financial market is the result of the complex interplay of various factors such as the sentiment of market participants, information dissemination, and macroeconomic fundamentals. Generally, markets are either order-driven or quotes-driven with hybrid arrangements also possible. Typically, order-driven markets function through a limit order book, whereas quotes-driven markets function through a dealer.

In order-driven markets, such as many stock exchanges, prices are determined by the matching of buy and sell orders submitted by market participants. A limit order specifies a direction (buy or sell), a quantity, and a price at which the transaction should be executed. From a seller's perspective, the limit order price is the minimal price, one is willing to sell the asset for, and conversely from the buyer's perspective. The collection of all placed limit orders is the limit order book, and when a new order arrives in the market, it is compared to the existing orders in the book. If the order is compatible with one or more orders in the book, then a transaction takes place. A buy order gets executed at the best (lowest) available ask quote, and then walks the order book to obtain the specified quantity and complete the order. The last price at which the order gets executed becomes the quoted price of the asset. Each transaction is accompanied with a time stamp known as the transaction time. These recorded transactions becomes the price series that we observe in the market. The difference between the bid quotes and the ask quotes is known as the bid-ask spread. The bid-ask spread is the de facto measure of market liquidity, since highly liquid assets will have an abundance of price takers and thus also a narrow bid-ask spread.

Alternatively, quotes-driven markets function through a dealer, which lists the bid and ask quotations available to investors.

2.2 Jumps and Asynchronicity

In most cases, both limit order markets and dealers markets operate continuously during the opening hours with no activity during the closing hours. Consequently, large price increments will be recorded from the previous close to the next opening due to the cumulative effect of the information revealed overnight. Statistics based on the price increments would then generate an additional jump every morning, which is contradictory to the usual notion

of jumps arriving at random and unpredictable times. A statistical model of the asset prices incorporating jumps would have to take this into consideration.

Another major distinction from standard time series data is that observations are not equally spaced, since transactions can occur at any time during opening hours. Furthermore, the trading volume of the asset varies throughout the trading day with some periods of higher trading intensity and also more observations. Obtaining a series of equally spaced prices therefore requires making some assumptions.

If more assets are traded, then the transactions might not occur simultaneously resulting in asynchronous data. Additionally, transaction times are rounded to the nearest second, whereas traders operate on a millisecond scale. Consequently, multiple observations may occur simultaneously resulting in a loss of clear time-sequencing.

2.3 Microstructure Noise

A major characteristic of high-frequency financial data is the presence of microstructure noise, i.e. the observations are contaminated with noise, which interacts with the sampling frequency in complicated ways. We think of the log-prices of the assets as the prices corresponding to a perfect market with no trading imperfections, market friction, or informational asymmetries. The microstructure noise is then the discrepancy between this efficient log-price and the actual observed prices. This noise is a result of the trading process and can either be information or non-information related. The noise is caused by several factors such as the presence of bid-ask spread and the corresponding bounces, discreteness of prices, and informational asymmetries between traders.

If we let X denote the unobservable efficient log-price of a single asset, then we will assume that we observe the price process Y given by

$$Y_{\tau_i} = X_{\tau_i} + \varepsilon_{\tau_i}, \tag{2.1}$$

where $\tau_i := i\Delta_n$ with $\Delta_n := T/n$ is an equidistant time grid of our observation interval $[0, T]$ with $T > 0$. In this simple set-up here, we assume that the noise terms ε_{τ_i} are i.i.d. with $\mathbb{E}[\varepsilon_{\tau_i}] = 0$ and $\mathbb{E}[\varepsilon_{\tau_i}^2] = \psi > 0$, and that the noise process is independent of X. Note that this additive form of noise is far from the only way to specify the noise process.

Since our interest lie in the process X, we would like to mitigate the impact of the microstructure noise before conducting any further analysis on our data. High-frequency data are often available every second or every few seconds. It has been observed that microstructure noise is linked to each transaction and not the time separating successive transactions. Furthermore, the volatility of the efficient log-price process X and the market microstructure noise ε tend to exhibit different behaviour at different frequencies. Log-returns observed from transaction prices over a small time interval is mostly composed of microstructure noise and is not very informative regarding the volatility of X, since the volatility of the price process is proportional to the time interval separating successive observations. At least this is true for the case, where the volatility of the price process is driven by a Brownian motion.

Consequenly, very high-frequency data is mostly composed of market microstructure noise, and thus the informational content decreases drastically. The simplest method to mitigate this effect is simply to sample at lower frequency, so-called downsampling. In the literature, the sampling frequency is usually measured in minutes with 5 and 15 minute time interval often being employed. The disadvantage of downsampling is that potentially large amounts of data get discarded.

2.3.1 Data Example

As a preliminary data example, we consider the SPDR S&P 500 ETF Trust (SPY), which is the oldest and most popular exchange traded fund tracking the S&P 500 index. [30] For this subsection, we consider the intradaily data of January 4th 1999, which amounts to 2036 transactions recorded between from 9:32:31 UTC to 16:16:27 UTC. Initially, we disgard transactions recorded after 16:00:00 UTC, since these are transactions recorded past opening hours, which means we get 2004 observations in total. The price series is plotted in Figure 2.1.

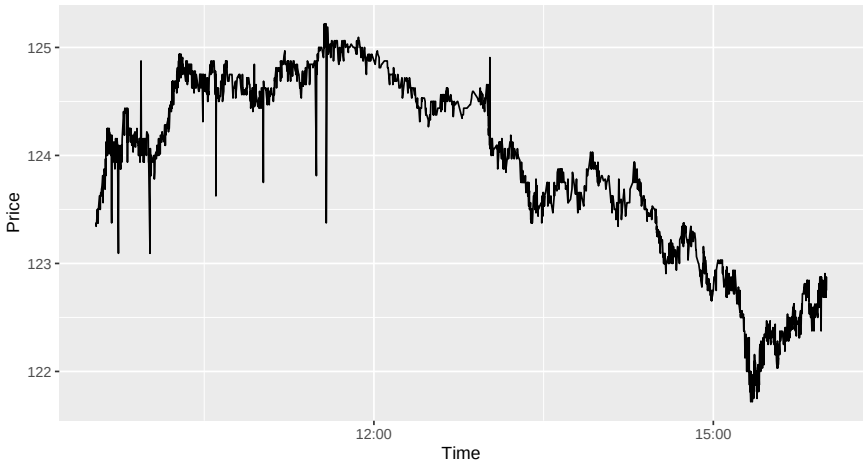

Figure 2.1: *SPY ETF, January 4th 1999*

The data exhibits many of the previously discussed characteristics for high-frequency data. The data is asynchronous with periods of varying trading intensity as exhibited in Figure 2.2. The times between observations span between 0 seconds to 137 seconds with 75% of the arrival times being less than or equal to 15 seconds. The blue curve is a kernel density estimate computed from the data using a Gaussian kernel on a grid spanning from $t = 0$ to $t = 137$. The orange curve is the exponential density function with rate parameter equal to the maximum likelihood estimate

$$\hat{\lambda}_n = \frac{n}{\sum_{i=1}^{n} t_i} \tag{2.2}$$

computed from the times recorded between transactions $t_1, t_2, \ldots, t_n$. Clearly, the distribution of arrival times is heavily right-skewed. Furthermore, the kernel density estimate and the exponential density seem to agree, which indicates that a Poisson point process might be a good fit for modelling transaction times.

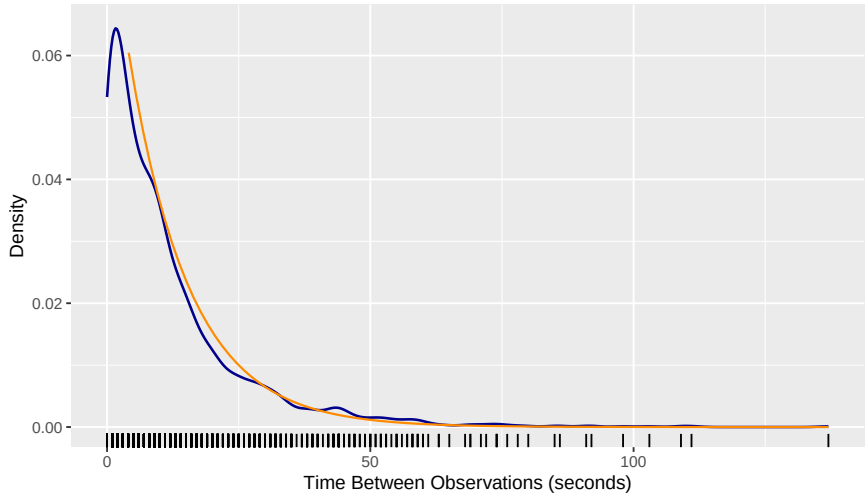

Figure 2.2: *Times between Transactions, Kernel Density (blue), and Exponential Density (orange).*

One way to deal with asynchronicity and microstructure noise is sampling at lower frequencies on an equidistant time grid. In order to create a series of equally spaced values with inter-observation time Δ, some assumptions are neccesary. If no transaction is recorded at time $i\Delta$, we take the last recorded price previous to $i\Delta$. In order for this to be efficient, Δ must be at least slightly longer than the average time separating the actual transactions. In Figure 2.3, the price series in Figure 2.1 is sampled with Δ being 30 seconds, 1 minute, and 5 minutes, respectively.

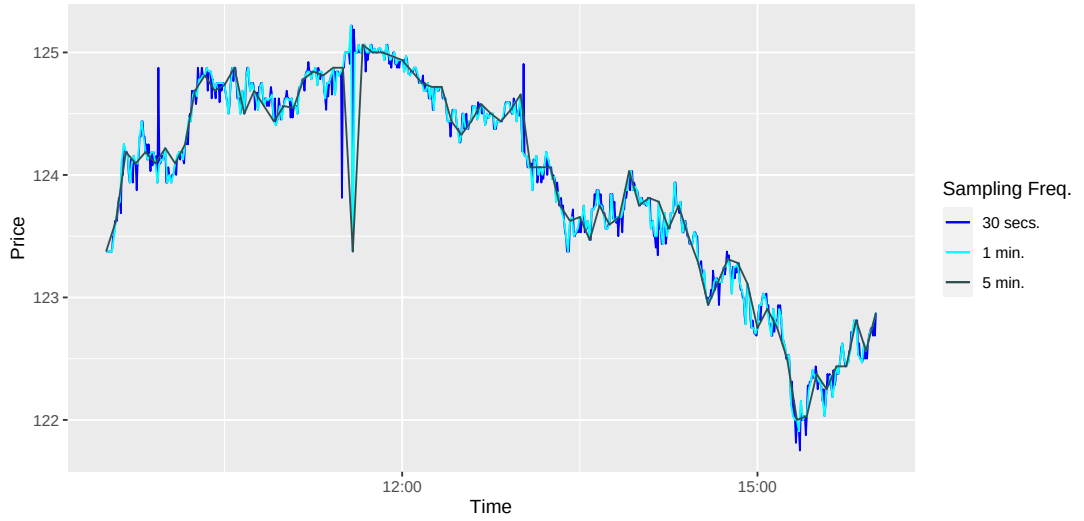

Figure 2.3: *Price Series Sampled at 30 Second, 1 Minute, and 5 Minute Frequencies.*

However, it is important to note that we lose substantial amounts of data. Sampling at 30 seconds leaves us with 781 transactions, 1 minute sampling leaves 391 transactions, and 5 minute sampling leaves 79 observations. Sampling at 30 seconds preserves a lot of the information contained in Figure 2.1 including various spikes, whereas 5 minute sampling preserves the overall trend in the original price series.

Another distinct characteristic of high-frequency financial data is the non-normality

of log-returns, which especially suggests a departure from the Brownian-only paradigm prevalent in the financial mathematics literature.

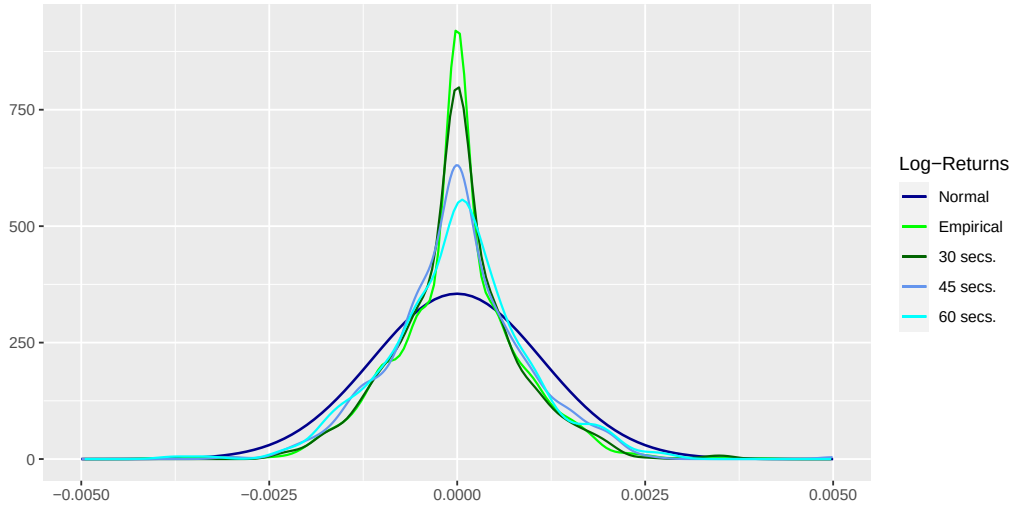

Figure 2.4: *Marginal Densities for Log-Returns at Different Frequencies.*

As evident in Figure 2.4, the log-returns strongly deviate from a normal distribution. The fitted normal density $\hat{f} \sim \mathcal{N}(\hat{\mu}, \hat{\sigma})$ with the sample mean and sample standard deviation computed from the log-returns is plotted in Figure 2.4 along with the marginal density of the log-returns. Furthermore, the marginal densities of log-returns at 30, 45, and 60 second frequencies are also shown. The non-normality is clearly visible at all frequencies.

3 Estimation of Integrated Volatility

In this section, we introduce the important concept of the quadratic variation of a semimartingale. We introduce the first model for log-prices and investigate how the realized covariation estimator can be used to estimate the integrated volatility within this set-up.

3.1 Itô Semimartingales

This section is based on [2, p. 10-40]

Definition 3.1 (*Semimartingale*)**.**
Let $X = (X_t)_{t\geqslant 0}$ be a stochastic process defined on the filtered probability space $(\Omega, \mathcal{F}, (\mathcal{F}_t)_{t\geqslant 0}, \mathbb{P})$. Then X is called a semimartingale if it admits the decomposition

$$X_t = X_0 + A_t + M_t, \quad t \geqslant 0, \tag{3.1}$$

where A is a cádlág process with finite local variation, and M is a cádlág local martingale. Additionally, it must hold that $A_0 = M_0 = 0$.

The process A has finite local variation, which means that the total variation of each path $t \mapsto A_t(\omega)$ is finite on each interval $[0, T]$ for $T > 0$. Furthermore, if X is continuous, then so is A and M. The processes A and M are unique up to indistinguishability, i.e. if $X_t = X_0 + \tilde{A}_t + \tilde{M}_t$ for another pair $(\tilde{A}, \tilde{M})$, then A and $\tilde{A}$ as well as M and $\tilde{M}$ are indistinguishable processes.

We recall that a local martingale M admits the unique decomposition

$$M = M_0 + M_t^c + M_t^d, \tag{3.2}$$

where $M_0^c = M_0^d = 0$, M^c is a continuous local martingale, and M^d is a local martingale orthogonal to all continuous local martingales, meaning that MN is a local martingale for any continuous local martingale N. We say that M^d is purely discontinuous although this does not refer to the sample path behaviour of M^d. Utilizing (3.2), we can rewrite the decomposition of the semimartingale X as

$$X_t = X_0 + X_t^c + M_t + A_t, \tag{3.3}$$

where $A_0 = M_0 = 0$, M is purely discontinuous local martingale, and X^c is a continuous local martingale starting at 0. Note that in (3.3), the processes M and A are still not unique, but X^c is unique and is called the continuous local martingale part of X.

Additionally, for a semimartingale X, we can associate its jump process defined as

$$\Delta X_t := X_t - \lim_{s \to t^-} X_s, \tag{3.4}$$

where by convention $\Delta X_0 = 0$. The limit in (3.4) is taken from the left due to the assumption of X being cádlág. Another pertinent property of semimartingales is that they are the largest class of processes for which the quadratic variation exists.

Definition 3.2 (*Quadratic Variation*)**.**
Let $\mathcal{P} := \{0 = t_0 < t_1 < \cdots < t_n = t\}$ be a partition of $[0, t]$, and let $|\mathcal{P}| := \sup_{1 \leqslant i \leqslant n} |t_i - t_{i-1}|$. Then we define the quadratic variation of the d-dimensional semimartingale X as

$$\langle X \rangle_t = \mathbb{P} - \lim_{|\mathcal{P}| \to 0} \sum_{i=1}^{n} (X_{t_i} - X_{t_{i-1}})(X_{t_i} - X_{t_{i-1}})^\top. \tag{3.5}$$

For a one-dimensional semimartingale X, we may write its quadratic variation as

$$\langle X \rangle_t = \langle X^c \rangle_t + \sum_{s \leqslant t} (\Delta X_s)^2, \tag{3.6}$$

where the sum above makes sense, since the set $\{s : \Delta X_s \neq 0\} \cap [0, t]$ is countable. Hence, the quadratic variation of X is equal to the quadratic variation of the continuous local martingale X^c plus the sum of the squared jumps of X until time t.

For our puposes, we will consider a particular class of semimartingales.

Definition 3.3 (*Continuous Itô Semimartingale*)**.**
A d-dimensional semimartingale $X = (X_t)_{t \geqslant 0}$ supported by $(\Omega, \mathcal{F}, (\mathcal{F}_t)_{t \geqslant 0}, \mathbb{P})$ is a continuous Itô semimartingale, if it can be written as

$$X_t = X_0 + \int_0^t b_s ds + \int_0^t \sigma_s dB_s, \tag{3.7}$$

where X_0 is $\mathcal{F}_0$-measurable, B is a q-dimensional standard Brownian motion, $(b_t)_{t \geqslant 0}$ and $(\sigma_t)_{t \geqslant 0}$ are $\mathbb{R}^d$-valued and $\mathbb{R}^{d \times q}$-valued progressively measurable processes satisfying $\int_0^t \|b_s\| ds < \infty$ and $\int_0^t \|\sigma_s^2\| ds < \infty$ for all $t \in [0, \infty)$, respectively.

In the modelling of high-frequency financial data, a d-dimensional Itô semimartingale $X = (X^{(1)}, X^{(2)}, \ldots, X^{(d)})^\top$ defined on some compact interval $I_T := [0, T]$ for $T > 0$ is used as our model of the log-prices of some asset S, i.e. $X_t = \log S_t$.[1] In this setup, we will be interested in the non-parametric estimation of the so-called integrated volatility of the price process defined as

$$C_t := \int_0^t c_s ds, \quad c_s := \sigma_s \sigma_s^\top, \quad t \in I_T, \tag{3.8}$$

where $c = (c_t)_{t \in I_T}$ is the spot volatility, and the integrated volatility C_t is a matrix comprised of the aggregated volatility levels during the time interval I_t. Note however, that since the volatility process σ_t is a latent variable, both c_t and C_t are also unobservable and thus can only be estimated trough the observed price series X_t. Henceforth, we assume that the time-horizon $T > 0$ is fixed. Furthermore, the following process, known as the integrated quarticity, will be useful in the following sections

$$C(4)_t := \int_0^t c_s^2 ds, \quad t \in I_T. \tag{3.9}$$

[1] For the remainder of the project report, we simply refer to log-prices as prices and log-returns as returns.

3.2 Realized Covariation

This section is based on [5].

If we consider the intra-daily returns of some one-dimensional price process X computed during the time interval I_t, i.e.

$$r_{i\Delta_n} \coloneqq X_{i\Delta_n} - X_{(i-1)\Delta_n}, \quad i = 1, \ldots, n, \tag{3.10}$$

where n is the number of time intervals used in the computation, and $\Delta_n \coloneqq t/n$ is the spacing of the equidistant grid. Then we define the realized variance for X during I_t as

$$RV_t^{(n)} \coloneqq \sum_{i=1}^{n} r_{i\Delta_n}^2. \tag{3.11}$$

For a price process X given by a Itô semimartingale of the form (3.7), the realized variance is a consistent estimator of the integrated volatility

$$RV_t^{(n)} \xrightarrow{\mathbb{P}} \int_0^t \sigma_s^2 ds \quad \text{as} \quad n \to \infty. \tag{3.12}$$

Furthermore, we have the following central limit theorem (CLT) for the realized variance

$$\sqrt{n}\frac{RV_t^{(n)} - \int_0^t \sigma_s^2 ds}{\sqrt{2t\int_0^t \sigma_s^4 ds}} \xrightarrow{d} \mathcal{N}(0,1) \quad \text{as} \quad n \to \infty. \tag{3.13}$$

The CLT (3.13) enables us to construct confidence bands for the integrated volatility.

The realized variance will be our first estimator of the integrated volatility C_T. However, even though the realized variance nomenclature is standard in econometric literature, we will instead adopt the realized covariation nomenclature, since this is more accurate. Futhermore, as an intial simplification, we assume that no microstructure noise is present, and that X is sampled equidistantly at times $i\Delta_n$ for $i = 0, 1, \ldots, \lfloor T/\Delta_n \rfloor$, where the mesh $\Delta_n \to 0$ as $n \to \infty$. We now define the realized covariation $\widehat{C}(\Delta_n)_t$ by

$$\widehat{C}(\Delta_n)_t \coloneqq \sum_{i=1}^{\lfloor t/\Delta_n \rfloor} (\Delta_i^n X)^2, \quad \text{where} \quad \Delta_i^n X \coloneqq X_{i\Delta_n} - X_{(i-1)\Delta_n}. \tag{3.14}$$

If a semimartingale contains no jumps, then the quadratic variation equals the integrated volatility. Since X is assumed to be a continuous Itô semimartingale, this is the case here, and we have the following convergence

$$\widehat{C}(\Delta_n)_t \xrightarrow{\mathbb{P}} \langle X \rangle_t \quad \text{as} \quad \Delta_n \to 0. \tag{3.15}$$

3.2.1 Realized Covariation in the Presence of Noise

This section is based on [2, p. 209-218].

We will now relax the assumption of the observed price process containing no noise. How to specify the actual form of the noise and circumvent its effects are topics that have been studied extensively in the literature on microstructure noise. In the following, we will investigate an additive white noise process, which is also the setting that has been studied the most within the literature. We thus have

$$Y_i^n = X_{i\Delta_n} + \varepsilon_i^n, \quad i = 0, 1, \ldots, \lfloor T/\Delta_n \rfloor. \tag{3.16}$$

The superscript n for Y_i^n indicates the sampling frequency. In this set-up, at each frequency n, the process $(\varepsilon_t^n)_{t\in I_T}$ is globally independent of X and has the form

$$\varepsilon_i^n = \alpha_n \xi_{i\Delta_n}, \tag{3.17}$$

where $\xi = (\xi_t)_{t\in I_T}$ is a white noise process. Furthermore, it is customary to assume that the random variables ξ_t has moments of all orders with the moment structure

$$\mathbb{E}[\xi_t] = 0, \quad \mathbb{E}[\xi_t^2] = \psi, \quad \forall t \in I_T, \tag{3.18}$$

where $\psi > 0$. The extension to a general d-dimensional white noise process is straightforward

$$\mathbb{E}[\xi_t] = 0, \quad \mathbb{E}[\xi_t \xi_t^\top] = \Psi, \quad \forall t \in I_T, \tag{3.19}$$

where Ψ is a $d \times d$-dimensional positive definite matrix.

In regards to α_n, two variants are possible. In the first, the law of ε_i^n does not depend on n, and we set $\alpha_n = 1$ for all frequencies n. Alternatively, the law of ε_i^n does depend on n and shrinks as n increases. In this case, we have so-called shrinking noise, i.e.

$$\alpha_n \to 0 \quad \text{as} \quad \Delta_n \to 0. \tag{3.20}$$

If we consider the realized covariation estimator in the presence of noise, the estimator becomes

$$\widehat{C}^{\text{noisy}}(\Delta_n)_t = \sum_{i=1}^{\lfloor t/\Delta_n \rfloor} (\Delta_i^n Y)^2. \tag{3.21}$$

Expanding out (3.21), we obtain

$$\begin{aligned} \widehat{C}^{\text{noisy}}(\Delta_n)_t = &\sum_{i=1}^{\lfloor t/\Delta_n \rfloor} (\Delta_i^n X)^2 + 2\alpha_n \sum_{i=1}^{\lfloor t/\Delta_n \rfloor} \Delta_i^n X(\xi_{i\Delta_n} - \xi_{(i-1)\Delta_n}) \\ &- 2\alpha_n^2 \sum_{i=1}^{\lfloor t/\Delta_n \rfloor} \xi_{(i-1)\Delta_n}\xi_{i\Delta_n} + \alpha_n^2 \sum_{i=1}^{\lfloor t/\Delta_n \rfloor} \big((\xi_{i\Delta_n})^2 + (\xi_{(i-1)\Delta_n})^2\big). \end{aligned} \tag{3.22}$$

The first term in (3.22) converges in probability to the quadratic variation $\langle X\rangle_t$ as $\Delta_n \to 0$. For the remaining terms, we use that ξ is a white noise process along with the Law of Large Numbers to obtain

$$2\alpha_n \sum_{i=1}^{\lfloor t/\Delta_n \rfloor} \Delta_i^n X(\xi_{i\Delta_n} - \xi_{(i-1)\Delta_n}) \xrightarrow{\mathbb{P}} 0, \tag{3.23}$$

$$2\alpha_n^2 \sum_{i=1}^{\lfloor t/\Delta_n \rfloor} \xi_{(i-1)\Delta_n}\xi_{i\Delta_n} \xrightarrow{\mathbb{P}} 0, \tag{3.24}$$

$$\Delta_n \sum_{i=1}^{\lfloor t/\Delta_n \rfloor} \big((\xi_{i\Delta_n})^2 + (\xi_{(i-1)\Delta_n})^2\big) \xrightarrow{\mathbb{P}} 2t\mathbb{E}[\xi_0^2], \tag{3.25}$$

as $\Delta_n \to 0$. The above holds unless $\Delta_n/\alpha_n^2 \to \infty$, i.e. α_n^2 must not converge to 0 faster than Δ_n. From the preceding, we infer the asymptotic behaviour of $\widehat{C}^{\text{noisy}}(\Delta_n)_T$

$$\Delta_n/\alpha_n^2 \to 0 \quad \Rightarrow \quad \frac{\Delta_n}{\alpha_n^2}\widehat{C}^{\text{noisy}}(\Delta_n)_T \xrightarrow{\mathbb{P}} 2T\mathbb{E}[\xi_0^2], \tag{3.26}$$

$$\Delta_n/\alpha_n^2 \to \theta \quad \Rightarrow \quad \widehat{C}^{\text{noisy}}(\Delta_n)_T \xrightarrow{\mathbb{P}} \langle X\rangle_T + \frac{2T}{\theta}\mathbb{E}[\xi_0^2], \tag{3.27}$$

$$\Delta_n/\alpha_n^2 \to \infty \quad \Rightarrow \quad \widehat{C}^{\text{noisy}}(\Delta_n)_T \xrightarrow{\mathbb{P}} \langle X\rangle_T, \tag{3.28}$$

where $\theta \in (0, \infty)$. Hence, in the case of (3.26), the realized covariation tends to ∞ at rate $1/\Delta_n$, when the noise size is constant ($\alpha_n = 1$), and at a slower rate when the noise shrinks too slowly. If the noise shrinks sufficiently fast as in (3.28), then the realized covariation will tend to the $\langle X \rangle_T$ as in the case without noise. Finally, there is an intermediary situation in (3.27), where the limit involves both $\langle X \rangle_T$ and the noise.

As an example, we consider a geometric Brownian motion

$$S_t = S_0 \exp\left\{\left(\mu - \frac{\sigma^2}{2}\right)t + \sigma B_t\right\}, \tag{3.29}$$

with $S_0 = 100$, $\mu = \sigma = 0.01$, and B_t is a standard Brownian motion. We simulate the process on $[0, 1]$ to emulate one trading day, and then set $X_t := \log S_t$. As our noise process, we simulate $\xi_i \overset{\text{i.i.d.}}{\sim} \mathcal{N}(0, 10^{-8})$ with constant noise size $\alpha_i = 1$ for all i. We then apply the estimator $\widehat{C}^{\text{noisy}}(\Delta_n)_t$ to $Y_i^n = X_{i\Delta_n} + \xi_i^n$, where $i = 0, 1, \ldots, n$ with $n = \lfloor 1/\Delta_n \rfloor$.

To illustrate the divergence of the realized covariation, we make a so-called signature plot, where the horizontal axis is Δ_n, and the vertical axis is the realized covariation computed over the entire trading day.

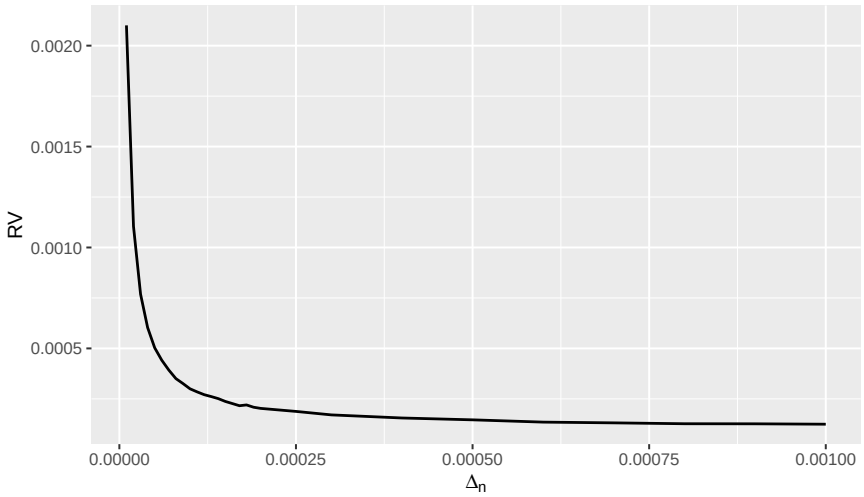

Figure 3.1: *Realized Covariation as a Function of* Δ_n.

We see that the realized covariation indeed tends to ∞ as $\Delta_n \to 0$ like a power law. An important conclusion from the plot above is that as sampling becomes more frequent, microstructure noise also becomes more predominant. This seems to contradict the model of shrinking noise, which will consequently not be considered in the sequel.

3.2.2 Asymptotics in Case of Constant Volatility

In this subsection, we will consider how to derive the asymptotic behaviour of the realized covariation estimator in the simple setting of a one-dimensional Itô semimartingale of the form

$$X_t = X_0 + \int_0^t \sigma_s dB_s, \quad t \in I_T. \tag{3.30}$$

Furthermore, we will assume that no microstructure noise is present along with constant volatility $\sigma_t = \sigma$. Hence, the integrated volatility to be estimated amounts to $C_T = Tc$, where $c = \sigma^2$. In this case, we are in a classical parametric setting with the parameter

$\theta = Tc$. The initial value X_0 does not influence the estimation of C_T, and thus we assume without loss of generality that $X_0 = 0$. Then at stage n, we observe $\lfloor T/\Delta_n \rfloor$ i.i.d. returns of the form $\Delta_i^n X \sim \mathcal{N}(0, c\Delta_n)$. The normality follows from the normality of the increments of a Brownian motion.

As in standard parametric statistics, we have a family of probability measures $\mathbb{P}_\theta$ indexed by θ, which are defined on the space $\mathbb{R}^{\mathbb{N}}$. At each stage n, the measures $\mathbb{P}_\theta$ restricted to the σ-algebra generated by the first $\lfloor T/\Delta_n \rfloor$ variables are equivalent to the Lebesgue measure on $\mathbb{R}^{\lfloor T/\Delta_n \rfloor}$. Consequently, the likelihood function exists, and the log-likelihood is given by

$$\ell_n(\theta) = -\frac{1}{2} \sum_{i=1}^{\lfloor T/\Delta_n \rfloor} \left(\frac{(\Delta_i^n X)^2}{c\Delta_n} + \log(2\pi c \Delta_n) \right), \tag{3.31}$$

where the MLE-estimate is given by

$$\hat{\theta}_n = \frac{T/\Delta_n}{\lfloor T/\Delta_n \rfloor} \widehat{C}(\Delta_n)_T. \tag{3.32}$$

The MLE is essentially just the realized covariation, but with the factor $\frac{T/\Delta_n}{\lfloor T/\Delta_n \rfloor} \geqslant 1$, which is an adjustment for the end point of the interval $[0, T]$, since T/Δ_n is not necessarily an integer. In practice, T/Δ_n is most often an integer, and even when this isn't the case, using the unbiased MLE-estimator $\hat{\theta}_n$ does not substantially improve estimation except for very small samples.

Employing $\widehat{C}(\Delta_n)_T$ instead of $\hat{\theta}_n$, we get that the normalized estimation errors are given by

$$\frac{1}{\sqrt{\Delta_n}} \left(\widehat{C}(\Delta_n)_T - C_T \right) = \frac{1}{\sqrt{\Delta_n}} \sum_{i=1}^{\lfloor T/\Delta_n \rfloor} \left(\left(\frac{\Delta_i^n X}{\sqrt{\Delta_n}} \right)^2 - c \right) - \frac{T - \Delta_n \lfloor T/\Delta_n \rfloor}{\sqrt{\Delta_n}} c. \tag{3.33}$$

The last term in (3.33) is a border adjustment term, and it simply equals 0, when T/Δ_n is an integer. Hence, we need to determine the distribution of the summands in (3.33) in order to derive the asymptotics. Since $\Delta_i^n X / \sqrt{\Delta_n} \sim \mathcal{N}(0, c)$, we have that

$$\mathbb{E}\left[\left(\frac{\Delta_i^n X}{\sqrt{\Delta_n}} \right)^2 - c \right] = \mathbb{E}\left[\left(\frac{\Delta_i^n}{\sqrt{\Delta_n}} \right)^2 \right] - c = 0, \tag{3.34}$$

$$\mathrm{Var}\left[\left(\frac{\Delta_i^n X}{\sqrt{\Delta_n}} \right)^2 - c \right] = \mathbb{E}\left[\left(\frac{\Delta_i^n X}{\sqrt{\Delta_n}} \right)^4 \right] + c^2 - 2c^2. \tag{3.35}$$

Whence, it only remains to compute the fourth moment of $\Delta_i^n X / \sqrt{\Delta_n}$ in order to derive the variance. Since $\Delta_i^n X / \sigma\sqrt{\Delta_n} \sim \mathcal{N}(0, 1)$, we have $(\Delta_i^n X / \sigma\sqrt{\Delta_n})^2 \sim \chi^2(1)$, from which we deduce that

$$\mathrm{Var}\left[\left(\frac{\Delta_i^n X}{\sigma\sqrt{\Delta_n}} \right)^2 \right] = 2 = \mathbb{E}\left[\left(\frac{\Delta_i^n X}{\sigma\sqrt{\Delta_n}} \right)^4 \right] - \mathbb{E}\left[\left(\frac{\Delta_i^n X}{\sigma\sqrt{\Delta_n}} \right)^2 \right]^2 \tag{3.36}$$

$$= \mathbb{E}\left[\left(\frac{\Delta_i^n X}{\sigma\sqrt{\Delta_n}} \right)^4 \right] - 1. \tag{3.37}$$

Hence, we have

$$\mathbb{E}\left[\left(\frac{\Delta_i^n X}{\sigma\sqrt{\Delta_n}} \right)^4 \right] = \frac{1}{c^2} \mathbb{E}\left[\left(\frac{\Delta_i^n X}{\sqrt{\Delta_n}} \right)^4 \right] = 3. \tag{3.38}$$

Substituting into (3.35), we obtain that the variance is

$$\mathrm{Var}\left[\left(\frac{\Delta_i^n X}{\sqrt{\Delta_n}}\right)^2 - c\right] = 2c^2. \tag{3.39}$$

By application of the central limit theorem to the centered i.i.d. summands in (3.33), we obtain the convergence

$$\frac{1}{\sqrt{\Delta_n}}\Big(\widehat{C}(\Delta_n)_T - C_T\Big) \xrightarrow{d} \mathcal{N}(0, 2C(4)_T). \tag{3.40}$$

However, the variance of the asymptotic distribution depends on the unknown quarticity $C(4)_T$. In order to construct confidence intervals for C_T, we need to estimate $2C(4)_T$, which can be done with

$$V_T^n := 2T(\widehat{C}(\Delta_n)_T)^2 \tag{3.41}$$

In this set-up with constant volatility, we have that

$$V_T^n \xrightarrow{\mathbb{P}} 2Tc^2 \quad \text{as} \quad \Delta_n \to 0, \tag{3.42}$$

i.e. V_T^n converges in probability to a constant. An application of Slutsky's Theorem, see Theorem A.2, now finally yields

$$\frac{\widehat{C}(\Delta_n)_T - C_T}{\sqrt{\Delta_n V_T^n}} \xrightarrow{d} \mathcal{N}(0,1). \tag{3.43}$$

Based on this, we can construct the following approximate $(1-\alpha)$-confidence interval for C_T

$$\Big[\widehat{C}(\Delta_n)_T - \Phi_{\alpha/2}\sqrt{\Delta_n V_T^n},\ \widehat{C}(\Delta_n)_T + \Phi_{1-\alpha/2}\sqrt{\Delta_n V_T^n}\Big], \tag{3.44}$$

where Φ_α is the α-quantile of the standard normal distribution. This is of course in agreement with the CLT in (3.13) as expected.

4 Testing for Jumps

One important aspect of high-frequency financial data, which the modelling in the previous chapter does not address, is the presence of jumps in the price series. In the previous chapter, we assumed that the price series was a continuous Itô semimartingale, which contains a drift component and a volatility component driven by a Brownian motion and has no jumps. If we relax the assumption of continuity, we can model the price series as a general Itô semimartingale, which can contain jumps. In particular, we will study the Lévy-Itô decomposition of a general semimartingale and the Grigelionis form of an Itô semimartingale. The Grigelionis form decomposes an Itô semimartingale as a drift component and a volatility component driven by a Brownian motion plus two jump components. The first jump component accounts for the small jumps of the process, while the second component accounts for the big jumps of the process.

Firstly, we present some preliminary definitions from measure theory, which are based on [12, p. 77-79].

Definition 4.1 (*Random Measure*)**.**
Let $(\Omega, \mathcal{F}, \mathbb{P})$ be a probability space and $(S, \mathcal{X})$ a measurable space. A random measure is a mapping $\zeta : \Omega \times \mathcal{X} \to [0, \infty]$ such that

1. For $\omega \in \Omega$, $\zeta(\omega, \cdot)$ is a measure on $(S, \mathcal{X})$.
2. For $B \in \mathcal{X}$, $\zeta(\cdot, B)$ is $\mathcal{F}$-measurable.

According to Definition 4.1, a random measure is a random variable, which takes its values in the set of measures on $(S, \mathcal{X})$. Before introducing the important concept of a Poisson random measure, we recall that for $E \subset \mathbb{R}^d$, a Radon measure μ on $(E, \mathcal{X})$ is a measure for which $\mu(B) < \infty$ for every compact set $B \in \mathcal{X}$.

Definition 4.2 (*Poisson Random Measure*)**.**
Let $(\Omega, \mathcal{F}, \mathbb{P})$ be a probability space, $E \subset \mathbb{R}^d$, and let μ be a Radon measure on $(E, \mathcal{X})$. A random measure $\zeta : \Omega \times \mathcal{X} \to \mathbb{N}$ is called a Poisson random measure with intensity measure μ if

1. For almost all $\omega \in \Omega$, $\zeta(\omega, \cdot)$ is an integer-valued Radon measure on $(E, \mathcal{X})$.
2. For any measurable set $A \subset E$, $\zeta(\cdot, A) = \zeta(A) \sim \text{Poi}(\mu(A))$.
3. $\zeta(A_1), \ldots, \zeta(A_n)$ are independent for disjoint $A_1, \ldots, A_n \in \mathcal{X}$.

4.1 Lévy-Itô Decomposition of a Semimartingale

This section is based on [19, p. 29-32].

We recall the decomposition in (3.3) of a general d-dimensional semimartingale X supported by $(\Omega, \mathcal{F}, (\mathcal{F}_t)_{t \geqslant 0}, \mathbb{P})$ into a sum of an adapted finite variation process A, a purely

discontinuous local martingale M, and a unique continuous local martingale X^c. We now associate to X the following process

$$X'_t = X_t - X_0 - J_t, \quad \text{where} \quad J_t := \sum_{s \leqslant t} \Delta X_s \mathbb{1}_{\{\|\Delta X_s\| > 1\}}. \tag{4.1}$$

The sum defining J_t is finite for almost all ω and t, and the process J is clearly adapted, cádlág and of finite variation. Consequently, J is a semimartingale, and so is X'. Furthermore, the size of the jumps of X' satisfy $\|\Delta X'\| \leqslant 1$ by construction. In particular, this implies that there is a unique decomposition (up to null sets) of X' such that the process A in (3.3) is predictable and of finite variation. We may write this decomposition as

$$X'_t = X_0 + B_t + X^c_t + M_t, \tag{4.2}$$

where $B_0 = M_0 = 0$, B is predictable and of finite variation, M is a purely discontinuous local martingale, and X^c is the same process as in (3.3). This gives us the following unique decomposition of X

$$X_t = X_0 + B_t + X^c_t + M_t + \sum_{s \leqslant t} \Delta X_s \mathbb{1}_{\{\|\Delta X_s\| > 1\}}. \tag{4.3}$$

We now introduce the following set for a cádlág $\mathbb{R}^d$-valued process Y

$$\mathcal{D}(Y) := \{(\omega, t) \in \Omega \times [0, \infty) : \Delta Y_t(\omega) \neq 0\}. \tag{4.4}$$

For each $\omega \in \Omega$, the set $\mathcal{D}(Y)$ of jump times of Y is at most countable due to Y being cádlág, although typically it may be a dense subset of $[0, \infty)$. Using this notation, we now associate with X the following jump measure μ given by

$$\mu(\omega; \mathrm{d}t, \mathrm{d}x) = \sum_{(\omega,s) \in \mathcal{D}(X)} \delta_{\{(s, \Delta X_s(\omega))\}}(\mathrm{d}t, \mathrm{d}x), \tag{4.5}$$

where $\delta_{\{(t,x)\}}$ is the Dirac measure concentrated in $(t, x) \in [0, \infty) \times \mathbb{R}^d$. Thus, for each ω, $\mu(\omega; \cdot)$ is an integer-valued measure satisfying $\mu\big(\omega; \{0\} \times \mathbb{R}^d\big) = \mu(\omega; [0, \infty) \times \{0\}) = 0$ and such that $\mu(\omega; \{t\} \times \mathbb{R}^d) = 1$ if $(\omega, t) \in \mathcal{D}(X)$ and 0 otherwise.

For any Borel set $A \subset \mathbb{R}^d$, we can then define the following process

$$\big(\mathbb{1}_A \star \mu(\omega)\big)_t := \mu(\omega; (0, t] \times A) = \sum_{s \leqslant t} \mathbb{1}_A(\Delta X_s). \tag{4.6}$$

The process $\mathbb{1}_A \star \mu$ is non-decreasing and adapted, although it may assume the value ∞ at some time $t > 0$ or even at all times $t > 0$. However, if the set A has positive distance to 0 in the sense that $d(0, A) = \inf\{\|a\| : a \in A\} > 0$, then the process $\mathbb{1}_A \star \mu$ is cádlág, $\mathbb{N}$-valued, and with jumps of size 1 and hence also locally integrable. Consequently, it admits a predictable compensator, denoted by $\mathbb{1}_A \star \nu$, which is a predictable, increasing, locally integrable process that starts at 0.

Additionally, the mapping $A \mapsto (\mathbb{1}_A \star \mu)_t$ is σ-additive, and accordingly the mapping $A \mapsto (\mathbb{1}_A \star \nu)_t$ is almost surely σ-additive. The preceding discussion allows us to conclude that there exists a positive random measure $\nu(\omega; \mathrm{d}t, \mathrm{d}x)$ on $[0, \infty) \times \mathbb{R}^d$ such that

$$\big(\mathbb{1}_A \star \nu(\omega)\big)_t = \nu(\omega; (0, t] \times A), \quad \forall A \in \mathcal{B}(\mathbb{R}^d). \tag{4.7}$$

The measure ν is called the predictable compensator of μ.

We may extend this notion to more general integrands than just indicator functions. If $\kappa : \Omega \times [0,\infty) \times \mathbb{R}^d \to \mathbb{R}$ is a measurable function, we write

$$(\kappa \star \mu)_t = \int_{[0,t]\times\mathbb{R}^d} \kappa(\omega, s, x)\, \mu(\omega; \mathrm{d}s, \mathrm{d}x), \tag{4.8}$$

$$(\kappa \star \nu)_t = \int_{[0,t]\times\mathbb{R}^d} \kappa(\omega, s, x) \mu(\omega; \mathrm{d}s, \mathrm{d}x). \tag{4.9}$$

In particular, the first integral (4.8) amounts to

$$(\kappa \star \mu)_t = \sum_{s\leqslant t} \kappa(s, \Delta X_s), \tag{4.10}$$

where we have suppressed the ω-dependency.

The following remarks are pertinent.

1. We can now define the so-called characteristics of a semimartingale X, which consist of a triplet (B, C, ν), where
   (a) $B = \left(B^i\right)_{i=1}^d$ is the predictable process of finite variation in (4.3).
   (b) $C = \left(C^{ij}\right)_{i,j=1}^d$, where $C^{ij} = \langle X^{i,c}, X^{j,c}\rangle$ is the quadratic variation of the i-th and j-th component of the continuous local martingale X^c.
   (c) ν is the compensator of the jump measure μ associated to X.

2. For any fixed ω, the integrals (4.8) and (4.9) are Lebesgue integrals with respect to the positive measures μ and ν. The measure $\mu - \nu$ is a signed measure, and furthermore it is a martingale measure in the sense that if the Borel set $A \subset \mathbb{R}^d$ has positive distance to 0, then $\mathbb{1}_A \star (\mu - \nu)$ is a local martingale. Consequently, we have a notion of a stochastic integral with respect to $\mu - \nu$.

3. We say a function κ on $\Omega \times [0,\infty) \times \mathbb{R}^d$ is predictable, if it is $\widetilde{\mathcal{P}}$-measurable, where $\widetilde{\mathcal{P}} := \mathcal{P} \otimes \mathcal{B}(\mathbb{R}^d)$ with $\mathcal{P}$ being the predictable σ-algebra on $\Omega \times [0,\infty)$. If κ is such a predictable function, which furthermore satisfies

   $$\left((\kappa^2 \wedge |\kappa|) \star \nu\right)_t < \infty, \quad \forall t > 0, \tag{4.11}$$

   then we can define a new process, which we denote by

   $$(\kappa \star (\mu - \nu))_t := \int_0^t \int_{\mathbb{R}^d} \kappa(\omega, s, x)\, (\mu - \nu)(\mathrm{d}s, \mathrm{d}x). \tag{4.12}$$

   We call (4.12) the stochastic integral of κ with respect to $\mu - \nu$.

4. Finally, having established this notion of stochastic integration with respect to $\mu - \nu$, we can present the final decomposition of a general semimartingale X

   $$X = X_0 + B + X^c + (x\mathbb{1}_{\|x\|\leqslant 1}) \star (\mu - \nu) + (x\mathbb{1}_{\|x\|>1}) \star \mu. \tag{4.13}$$

   This is called the Lévy-Itô decomposition of the semimartingale.

4.2 Grigelionis Form of an Itô Semimartingale

This section is based on [19, p. 35-38]

In Defintion 3.3, we defined a continuous Itô semimartingale as a continuous semimartingale taking the form (3.7). Having introduced the characteristics of a general semimartingale, we can now define a general Itô semimartingale, which need not be continuous.

Definition 4.3 (*Itô Semimartingale*)**.**
A d-dimensional semimartingale X is an Itô semimartingale, if its characteristics (B, C, ν) are absolutely continuous with respect to the Lebesgue measure in the sense that

$$B_t = \int_0^t b_s \, \mathrm{d}s, \quad C_t = \int_0^t c_s \, \mathrm{d}s, \quad \nu(\mathrm{d}t, \mathrm{d}x) = \mathrm{d}t \, F_t(\mathrm{d}x), \tag{4.14}$$

where $b = (b_t)_{t \geqslant 0}$ is a $\mathbb{R}^d$-valued process, $c = (c_t)_{t \geqslant 0}$ is a process with values in the set of $d \times d$ symmetric non-negative matrices, and $F_t = F_t(\mathrm{d}x)$ is a measure on $\mathbb{R}^d$ for every pair (ω, t).

We will now present the Grigelionis form of an Itô semimartingale. The original result is due to Grigelionis in [15], but the version presented below is from [17].

Theorem 4.4 (*Grigelionis Form*)**.**
Let X be a d-dimensional Itô semimartingale supported by $(\Omega, \mathcal{F}, (\mathcal{F}_t)_{t \geqslant 0}, \mathbb{P})$ with characteristics (B, C, ν) as in (4.14). Furthermore, d' is an integer with $d' \geqslant d$, E is an arbitrary Polish space with a finite or σ-finite measure λ, which has no atoms. Then one can construct a very good filtered extension $(\widetilde{\Omega}, \widetilde{\mathcal{F}}, (\widetilde{\mathcal{F}}_t)_{t \geqslant 0}, \widetilde{\mathbb{P}})$, which supports a d'-dimensional Brownian motion W and a Poisson random measure μ on $[0, \infty) \times E$ with intensity measure λ such that

$$X_t = X_0 + \int_0^t b_s \, \mathrm{d}s + \int_0^t \sigma_s \, \mathrm{d}W_s + (\kappa \mathbb{1}_{\|\kappa\| \leqslant 1}) \star (\mu - \nu)_t + (\kappa \mathbb{1}_{\|\kappa\| > 1}) \star \mu_t, \tag{4.15}$$

where $\nu(\mathrm{d}t, \mathrm{d}x) = \mathrm{d}t \otimes \lambda(\mathrm{d}x)$ is the compensator of μ, σ_t is an $\mathbb{R}^d \times \mathbb{R}^{d'}$-valued process on $(\Omega, \mathcal{F}, (\mathcal{F}_t)_{t \geqslant 0}, \mathbb{P})$, which is predictable, and κ is a predictable function on $\Omega \times [0, \infty) \times E$.

We refer to Section A.3 in Appendix A for details on Polish spaces and filtered extensions. Note that it is always possible to take $E = \mathbb{R}$ equipped with the Lebesgue measure λ. However, there is a lot of flexibility in choosing the extension, the space E, the function κ, and the dimension d'.

4.3 Ratio Test for Presence of Jumps

The rest of this chapter is based on [1].

In order to test for the presence of jumps, we will use the test proposed in [1], which utilizes a ratio of power variations as the test statistic. The only structural assumption is that the observed process X is an Itô semimartingale. Hence, we may write X_t in the Grigelionis form (4.15)

$$\begin{aligned} X_t = X_0 &+ \int_0^t b_s \, \mathrm{d}s + \int_0^t \sigma_s \, \mathrm{d}W_s + \int_0^t \int_E \kappa(\omega, s, x) \mathbb{1}_{\{\|\kappa\| \leqslant 1\}} (\mu - \nu)(\omega; \mathrm{d}s, \mathrm{d}x) \\ &+ \int_0^t \int_E \kappa(\omega, s, x) \mathbb{1}_{\{\|\kappa\| > 1\}} \nu(\omega; \mathrm{d}s, \mathrm{d}x), \end{aligned} \tag{4.16}$$

where the components in (4.16) are as in Theorem 4.4. Furthermore, the test assumes that σ_t is also an Itô semimartingale, which consequently admits the form

$$\begin{aligned}\sigma_t = \sigma_0 + \int_0^t \widetilde{b}\,\mathrm{d}s + \int_0^t \widetilde{\sigma}_s\,\mathrm{d}W_s + \int_0^t \widetilde{\sigma}'\,\mathrm{d}W'_s + \int_0^t \int_E \widetilde{\kappa}(\omega,s,x)\mathbb{1}_{\{\|\widetilde{\kappa}\|\leqslant 1\}}(\mu-\nu)(\omega;\mathrm{d}s,\mathrm{d}x) \\ + \int_0^t \int_E \widetilde{\kappa}(\omega,s,x)\mathbb{1}_{\{\|\widetilde{\kappa}\|>1\}}\nu(\omega;\mathrm{d}s,\mathrm{d}x),\end{aligned} \tag{4.17}$$

where W' is a Brownian motion independent of (W,μ). Furthermore, there are some additional technical assumptions on the drift components, volatility components and the functions κ and $\widetilde{\kappa}$, which we will not list here, but can be found in [1].

4.3.1 The Statistical Problem

We assume that we discretely observe a path $X(\omega)$ on some interval $[0,t]$ with the observations $i\Delta_n$ for $i = 0,1,\ldots,n$, where we only take into account the observation times less than or equal to t. Furthermore, the testing procedure is asymptotic in the sense that we specify the power of the test as $n \to \infty$ and $\Delta_n \to 0$.

We make the following comments.

1. The problem is non-parametric, i.e. we do not specify the forms of the coefficients b, σ or κ.

2. The problem is asymptotic, and hence it only makes sense for high-frequency data.

3. In the unrealistic case with $n = \infty$, where we observe a complete path $X(\omega)$ on $[0,t]$, we can of course determine whether there are jumps present or not. However, when the measure λ is finite there is a positive probability that the path $X(\omega)$ has no jumps on $[0,t]$ even though the model allows for jumps.

4. In the realistic case $n < \infty$, we cannot do better than the case when $n = \infty$. Thus, we can only infer something about the jumps that occur in our observed sample. We cannot infer anything about the jumps that the model may allow, but didn't occur on the interval $[0,t]$.

5. The test statistic is scale-invariant. If X is multiplied by an arbitrary constant, then the test statistic is unaffected. Furthermore, the limiting behaviour of the test statistic is independent of the dynamics of the process.

Consequently, the statistical problem consists of deciding which of the following complementary sets our path $X(\omega)$ belongs to based on the observations $X_{i\Delta_n}$

$$\Omega_t^j := \{\omega : s \mapsto X_s(\omega) \text{ is discontinuous on } [0,t]\}, \tag{4.18}$$

$$\Omega_t^c := \{\omega : s \mapsto X_s(\omega) \text{ is continuous on } [0,t]\}. \tag{4.19}$$

If we decide that the observed path belongs to Ω_t^j, then we also implicitly decide that model has jumps. However, if we instead decide on Ω_t^c, it does not mean that model is continuous, even on the interval $[0,t]$. Naturally, in both cases, we cannot say anything about what happens after time t.

4.3.2 The Test Statistic

Before we introduce the test statistic, we introduce the following two processes that both measure some kind of the variability of X

$$A(p)_t := \int_0^t |\sigma_s|^p \, \mathrm{d}s, \quad B(p)_t := \sum_{s \leqslant t} |\Delta X_s|^p, \quad p \in (0, \infty). \tag{4.20}$$

Note that $\langle X \rangle = A(2) + B(2)$. We have that $\Omega_t^j = \{B(p)_t > 0\}$ for any $p > 0$, and hence the testing problem essentially consists of determining whether $B(p)_t > 0$ for our observed path and for any p. Hence, we define the following natural estimator for $B(p)_t$

$$\widehat{B}(p, \Delta_n)_t := \sum_{i=1}^{\lfloor t/\Delta_n \rfloor} |\Delta_i^n X|^p. \tag{4.21}$$

For $r \in (0, \infty)$, we let m_r denote the rth absolute moment of a standard normal variable U, i.e.

$$m_r = \mathbb{E}[|U|^r] = \pi^{-1/2} 2^{r/2} \Gamma\left(\frac{r+1}{2}\right), \tag{4.22}$$

where $\Gamma(\cdot)$ denotes the Gamma function. We then have the following convergences in probability as $n \to \infty$

$$\begin{cases} \widehat{B}(p, \Delta_n)_t \xrightarrow{\mathbb{P}} B(p)_t, & p > 2, \\ \widehat{B}(p, \Delta_n)_t \xrightarrow{\mathbb{P}} \langle X \rangle_t, & p = 2, \\ \frac{\Delta_n^{1-p/2}}{m_p} \widehat{B}(p, \Delta_n)_t \xrightarrow{\mathbb{P}} A(p)_t, & p < 2. \end{cases} \tag{4.23}$$

Furthermore, if the process X is continuous, then $\frac{\Delta_n^{1-p/2}}{m_p} \widehat{B}(p, \Delta_n)_t \xrightarrow{\mathbb{P}} A(p)_t$ for any $p > 0$. We see that for $p > 2$, $\widehat{B}(p, \Delta_n)_t$ converges to $B(p)_t$, which is strictly positive if X has jumps, and the limit is independent of the sequence Δ_n. Moreover, when X is continuous, $\widehat{B}(p, \Delta_n)_t$ converges to $A(p)_t$. The limiting process $A(p)_t$ is independent of Δ_n, but the normalizing constant $\Delta_n^{1-p/2}/m_p$ does depend on Δ_n. This leads us to compare $\widehat{B}$ on two different Δ_n-scales, where we pick an integer $k \geqslant 2$, and then consider the ratio

$$\widehat{S}(p, k, \Delta_n)_t := \frac{\widehat{B}(p, k\Delta_n)_t}{\widehat{B}(p, \Delta_n)_t}. \tag{4.24}$$

Considering the limits in (4.23), we readily obtain the following result.

Theorem 4.5.
Let $t > 0$, $k \geqslant 2$, and $p > 2$. Then the random variables $\widehat{S}(p, k, \Delta_n)_t$ converge in probability to the variable $S(p, k)_t$ given by

$$S(p, k)_t := \begin{cases} 1, & \text{on the set } \Omega_t^j, \\ k^{p/2-1}, & \text{on the set } \Omega_t^c. \end{cases} \tag{4.25}$$

On the set Ω_t^c, the convergence holds for $p \leqslant 2$ as well.

Theorem 4.5 is not sufficient to construct a test, since we need a central limit theorem for our statistic $\widehat{S}$. As an auxiliary quantity, we introduce the following

$$D(p)_t := \sum_{s \leqslant t} |\Delta X_s|^p (\sigma_{s^-}^2 + \sigma_s^2), \tag{4.26}$$

where $p > 0$ and $\sigma_{s^-} := \lim_{u \to s^-} \sigma_u$.

We now have the following central limit theorem for the power variations.

Theorem 4.6 (*CLT for Power Variations*)**.**
Let $p > 3$. Then for any $t > 0$, we have for the pair of random variables that

$$\Delta_n^{-1/2}\big(\widehat{B}(p,\Delta_n)_t - B(p)_t, \widehat{B}(p,k\Delta_n)_t - B(p)_t\big) \xrightarrow{\mathcal{L}_s} \big(Z(p)_t, Z(p)_t + Z'(p,k)_t\big), \tag{4.27}$$

as $n \to \infty$, and where $Z(p)_t$ and $Z'(p,k)_t$ are defined on an extension $(\widetilde{\Omega}, \widetilde{\mathcal{F}}, (\widetilde{\mathcal{F}}_t)_{t\geqslant 0}, \widetilde{\mathbb{P}})$ of the original probability space $(\Omega, \mathcal{F}, (\mathcal{F}_t)_{t\geqslant 0}, \mathbb{P})$, and which conditionally on $\mathcal{F}$ have mean zero with $Z'(p,k)_t$ having the conditional variance

$$\widetilde{\mathbb{E}}[Z'(p,k)_t^2 \mid \mathcal{F}] = \frac{k-1}{2} p^2 D(2p-2)_t. \tag{4.28}$$

Moreover, if the processes X and σ have no common jumps, then Z' is $\mathcal{F}$-conditionally Gaussian.

If we in addition assume that X is continuous and let $p \geqslant 2$, then we have that

$$\Delta_n^{-1/2}\big(\Delta_n^{1-p/2}\widehat{B}(p,\Delta_n)_t - m_p A(p)_t,\, \Delta_n^{1-p/2}\widehat{B}(p,k\Delta_n)_t - k^{p/2-1} m_p A(p)_t\big) \tag{4.29}$$

converges stably in law to the bidimensional variable $(Y(p)_t, Y'(p,k)_t)$ defined on an extension $(\widetilde{\Omega}, \widetilde{\mathcal{F}}, (\widetilde{\mathcal{F}}_t)_{t\geqslant 0}, \widetilde{\mathbb{P}})$ of the original probability space $(\Omega, \mathcal{F}, (\mathcal{F}_t)_{t\geqslant 0}, \mathbb{P})$, and which conditionally on $\mathcal{F}$ is a centered Gaussian random variable with the covariance structure

$$\begin{aligned}
&\widetilde{\mathbb{E}}[Y(p)_t^2 \mid \mathcal{F}] = (m_{2p} - m_p^2) A(2p)_t,\\
&\widetilde{\mathbb{E}}[Y'(p,k)_t^2 \mid \mathcal{F}] = k^{p-1}(m_{2p} - m_p^2) A(2p)_t,\\
&\widetilde{\mathbb{E}}[Y(p)_t Y'(p,k)_t \mid \mathcal{F}] = (m_{k,p} - k^{p/2} m_p^2) A(2p)_t,
\end{aligned}$$

where

$$m_{k,p} = \mathbb{E}[|U|^p |U + \sqrt{k-1}V|^p], \tag{4.30}$$

for independent $U, V \sim \mathcal{N}(0,1)$.

In order for Theorem 4.6 to be useful, we need consistent estimator for $A(p)_t$ and $D(p)_t$. We need to estimate $D(p)_t$, when there are jumps in the process, and $A(p)_t$, when X is continuous. In order to estimate $A(p)_t$, we use a truncated realized pth variation. That is, for any $C > 0$ and $\varpi \in (0, 1/2)$, we have from [18] that if either $p = 2$, or $p > 2$ and X is continuous, then

$$\widehat{A}(p,\Delta_n)_t := \frac{\Delta_n^{1-p/2}}{m_p} \sum_{i=1}^{\lfloor t/\Delta_n \rfloor} |\Delta_i^n X|^p \mathbb{1}_{\{|\Delta_i^n X| \leqslant C\Delta_n^{\varpi}\}} \xrightarrow{\mathbb{P}} A(p)_t, \tag{4.31}$$

as $\Delta_n \to 0$.

Alternatively, one may use the realized multipower variations of [8]. For any $r \in (0, \infty)$ and an integer $q \geqslant 1$, we have from [7] that if X is continuous

$$\widetilde{A}(r,q,\Delta_n)_t := \frac{\Delta_n^{1-qr/2}}{m_r^q} \sum_{i=1}^{\lfloor t/\Delta_n - q + 1 \rfloor} \prod_{j=1}^{q} |\Delta_{i+j-1}^n X|^r \xrightarrow{\mathbb{P}} A(qr)_t. \tag{4.32}$$

Estimating $D(p)_t$ is more difficult, since we have to evaluate σ_s^2 and also evaluate $\sigma_{s^-}^2$ if s is a jump time. One possible way is to pick a sequence of integers k_n such that

$$k_n \to \infty \quad \text{and} \quad k_n \Delta_n \to 0 \tag{4.33}$$

as $n \to \infty$. We then let $I_{n,t}(i) := \{j \in \mathbb{N}\backslash\{i\} : 1 \leqslant j \leqslant \lfloor t/\Delta_n \rfloor, |i-j| \leqslant k_n\}$ be a local window of length $2k_n\Delta_n$ around $i\Delta_n$, and define the estimator

$$\widehat{D}(p,\Delta_n)_t := \frac{1}{k_n\Delta_n} \sum_{i=1}^{\lfloor t/\Delta_n \rfloor} |\Delta_i^n X|^p \sum_{j\in I_{n,t}(i)} (\Delta_j^n X)^2 \mathbb{1}_{\{|\Delta_j^n X| \leqslant C\Delta_n^{\varpi}\}}, \tag{4.34}$$

where $C > 0$ and $\varpi \in (0, 1/2)$.

Theorem 4 in [1] establishes the consistency of the estimator $\widehat{A}(p,\Delta_n)_t$ for $p \geqslant 2$, $t > 0$, $C > 0$, and $\varpi \in (\frac{1}{2} - \frac{1}{p}, \frac{1}{2})$. For $\widehat{D}(p,\Delta_n)_t$ consistency is established for $p > 2$, $t \geqslant 0$, $C > 0$, and $\varpi \in (0, 1/2)$.

We now have the following central limit theorem for our test statistic $\widehat{S}$.

Theorem 4.7 (*CLT for Test Statistic*)**.**
Let $p > 3$ and $t > 0$ and set

$$\widehat{V}_{n,t}^j = \Delta_n \frac{(k-1)p^2 \widehat{D}(2p-2,\Delta_n)_t}{2\widehat{B}(p,\Delta_n)_t^2}. \tag{4.35}$$

Then the variables $(\widehat{V}_{n,t}^j)^{-1/2}(\widehat{S}(p,k,\Delta_n)_t - 1)$ converge stably in law, in restriction to the set Ω_t^j, to a variable, which conditionally on $\mathcal{F}$ is centered with variance 1, and which is $\mathcal{N}(0,1)$ if X and σ have no common jumps.

If we in addition assume that X is continuous, then for $p \geqslant 2$ and $t > 0$, we have that the variables $(\widehat{V}_{n,t}^c)^{-1/2}(\widehat{S}(p,k,\Delta_n)_t - k^{p/2-1})$ converge stably in law to a variable, which is $\mathcal{N}(0,1)$ conditional on $\mathcal{F}$, where $\widehat{V}_{n,t}^c$ is given by

$$\widehat{V}_{n,t}^c = \Delta_n \frac{M(p,k)\widehat{A}(2p,\Delta_n)_t}{\widehat{A}(p,\Delta_n)_t^2}, \tag{4.36}$$

with

$$M(p,k) = \frac{1}{m_p^2}\Big(k^{p-2}(1+k)m_{2p} + k^{p-2}(k-1)m_p^2 - 2k^{p/2-1}m_{k,p}\Big). \tag{4.37}$$

4.3.3 Construction of the Test

We can now construct a test with the null hypothesis that no jumps occur during $[0,t]$

$$\mathcal{H}_0 : s \mapsto X_s(\omega) \text{ is continuous on } [0,t]. \tag{4.38}$$

We choose an integer $k \geqslant 2$ and $p > 3$ and associate the critical region, which takes the form

$$C_{n,t}^c = \Big\{\widehat{S}(p,k,\Delta_n)_t < c_{n,t}^c\Big\}, \tag{4.39}$$

where $c_{n,t}^c$, $n \in \mathbb{N}$, is some sequence, which may be $c_{n,t}^c = c_t^c$ for all $n \in \mathbb{N}$, or it may possibly be a random sequence. In order to construct an asymptotic test on level $\alpha \in (0,1)$, i.e. $\mathbb{P}(C_{n,t}^c) = \alpha_{n,t}^c(b,\sigma,\kappa)$, we should take the supremum of all triples (b,σ,κ) of possible coefficients in the null hypothesis ($\kappa \equiv 0$) of $\limsup_n \alpha_{n,t}^c(b,\sigma,\kappa)$. Note that we write $\alpha = \alpha_{n,t}^c(b,\sigma,\kappa)$ in order to stress the dependence on $n, t, c_{n,t}^c, b, \sigma$, and κ. As mentioned previously, there is no way to statistically distinguish the null hypothesis from the case, where model has jumps but none occurred in $[0,t]$. Therefore, we condition on the set Ω_t^c and define our asymptotic test level as

$$\alpha = \sup_{b,\sigma,\kappa} \limsup_{n\to\infty} \mathbb{P}(C_{n,t}^c \mid \Omega_t^c), \tag{4.40}$$

with the convention that $\mathbb{P}(\cdot \mid \Omega_t^c) = 0$ if $\mathbb{P}(\Omega_t^c) = 0$. Furthermore, the power function of the test is given by

$$\beta_{n,t}^c(b, \sigma, \kappa) = \mathbb{P}(C_{n,t}^c \mid \Omega_t^j). \tag{4.41}$$

The power function is thus the probability that we correctly reject the null hypothesis of no jumps conditional on the set Ω_t^j.

We conclude this chapter with the following proposition, which summarizes the test.

Proposition 4.8.
Let $t > 0$ and choose a real $p > 3$ and an integer $k \geqslant 2$. We then set

$$c_{n,t}^c = k^{p/2-1} - \Phi_\alpha \sqrt{\widehat{V}_{n,t}^c}, \tag{4.42}$$

where $\widehat{V}_{n,t}^c$ is given by (4.36) with $\varpi \in (\frac{1}{2} - \frac{1}{p}, \frac{1}{2})$, $C > 0$, and Φ_α is the α-quantile of a standard normal random variable for $\alpha \in (0, 1)$. The asymptotic test level (4.40) of the critical region defined by (4.39) for testing the null hypothesis $\mathcal{H}_0$ is then equal to α.

Furthermore, the power function satisfies that $\beta_{n,t}^c(b, \sigma, \kappa) \to 1$ as $\Delta_n \to 0$ for all coefficient triplets (b, σ, κ) such that $\mathbb{P}(\Omega_t^j) > 0$.

5 Stochastic Delay Differential Equations

In this chapter, we investigate so-called stochastic delay differential equations with additive noise, where the linear fractional stable motion constitutes the noise term. Hence, we firstly have a short introduction to stable distributions, which is followed by a section on the linear fractional stable motion and how to simulate it.

5.1 Stable Distributions

This section is based on [24, p. 1-13] and [28, p. 1-21].

Definition 5.1 (*Characteristic Function*)**.**
Let $X : (\Omega, \mathcal{F}, \mathbb{P}) \to (\mathbb{R}^d, \mathcal{B}(\mathbb{R}^d))$ be a random variable with distribution $\mu_X(A) = \mathbb{P}(X \in A)$, $A \in \mathcal{F}$. Then the characteristic function $\varphi_X : \mathbb{R}^d \to \mathbb{C}$ of X is given by

$$\varphi_X(u) = \mathbb{E}[e^{iu^\top X}] = \int_{\mathbb{R}^d} e^{iu^\top x} \mu_X(\mathrm{d}x). \tag{5.1}$$

If we have a continuous random variable X, which admits an expressible density function f, then the characteristic function may be written as

$$\varphi_X(u) = \int_{\mathbb{R}^d} e^{iu^\top x} f(x) \mathrm{d}x. \tag{5.2}$$

Note that the characteristic function of a random variable is proportional to the Fourier transform of its density function.

Definition 5.2 (*Stable Random Variable*)**.**
A non-degenerate random variable X is said to be stable, if for all $n \geqslant 2$ there exists constants $c_n > 0$ and $d_n \in \mathbb{R}$ such that

$$X_1 + \cdots + X_n \overset{\mathcal{L}}{=} c_n X + d_n, \tag{5.3}$$

where $X_1, \ldots, X_n$ are i.i.d. copies of X. X is said to be strictly stable if $d_n = 0$ for all n.

We have the following Theorem.

Theorem 5.3.
For any stable random variable X, there exists a unique $\alpha \in (0, 2]$ such that (5.3) holds with $c_n = n^{1/\alpha}$.

The proof of Theorem 5.3 is omitted. The number α is called the index of stability or characteristic exponent.

While Definition 5.2 is intuitively clear, it doesn't give a concrete way of parameterizing stable distributions. An equivalent definition is that a random variable X is stable, if its characteristic function φ_X can be written as

$$\varphi_X(u) = \begin{cases} \exp\{-\gamma^\alpha |u|^\alpha \big(1 - i\beta \operatorname{sgn}(u) \tan(\frac{\pi\alpha}{2})\big) + i\delta u\}, & \alpha \neq 1, \\ \exp\{-\gamma|u|\big(1 + i\beta \operatorname{sgn}(u) \frac{2}{\pi} \log|u|\big) + i\delta u\}, & \alpha = 1, \end{cases} \tag{5.4}$$

where $\operatorname{sgn}(\cdot)$ denotes the sign function. The parameters $\alpha \in (0, 2]$ and $\beta \in [-1, 1]$ are shape parameters, and $\gamma > 0$ and $\delta \in \mathbb{R}$ are scale and location parameters, respectively. We write $X \sim S(\alpha, \beta, \gamma, \delta)$, if X follows such a stable distribution. Note that (5.4) is only one possible parameterization with the disadvantage of being discontinuous in the α-parameter, since $\tan(\pi\alpha/2) \to \infty$ for $\alpha \to 1^-$ and $\tan(\pi\alpha/2) \to -\infty$ for $\alpha \to 1^+$.

In the case of $\beta = 0$, the characteristic function just becomes a streched exponential function

$$\varphi_X(u) = \exp\{-\gamma^\alpha |u|^\alpha + i\delta u\}. \tag{5.5}$$

Furthermore, the distribution of X is symmetric around δ when $\beta = 0$. Additionally, if $\delta = 0$, then the characteristic function is real $\varphi_X(u) = \overline{\varphi_X(u)}$ and symmetric $\varphi_X(u) = \varphi_X(-u)$. As is well-known from Fourier theory, X is then symmetric around 0 with an even density function.

All stable distributions are absolutely continuous distributions with a density function that is C^∞, see Theorem 1.1 in [24] for instance. However, only three stable distributions have a density that is expressible in closed-form, namely the normal, Cauchy, and Lévy distributions. When $\alpha = 2$ and $\beta = 0$, $S(2, 0, \gamma, \delta)$ is simply a normal random variable with mean $\mu = \delta$ and variance $\sigma^2 = 2\gamma^2$. If $\alpha = 1$ and $\beta = 0$, we have $S(1, 0, \gamma, \delta) \sim \text{Cauchy}(\gamma, \delta)$ with scale and location parameters $(\gamma, \delta) \in (0, \infty) \times \mathbb{R}$. Finally, if $\alpha = 1/2$ and $\beta = 1$, we have that $S(1/2, 1, \gamma, \delta) \sim \text{Lévy}(\gamma, \delta)$ is a Lévy distribution with scale and location parameters $(\gamma, \delta) \in (0, \infty) \times \mathbb{R}$ and support on (δ, ∞). The densities of the standard normal, Cauchy, and Lévy distributions are shown in Figure 5.1.

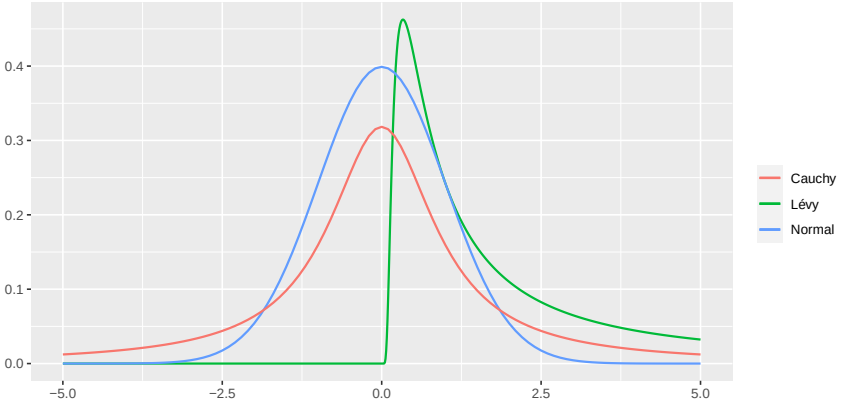

Figure 5.1: *Densities for Standard Normal, Cauchy*$(0, 1)$*, and Lévy*$(0, 1)$ *Distributions.*

It is clear from Figure 5.1 that the Cauchy and Lévy distributions have heavier tails than the normal distribution. In the Gaussian case $X \sim \mathcal{N}(\mu, \sigma^2)$, it is well-known that the tail probabilities decay exponentially

$$\lim_{x \to \infty} e^{\lambda x} \mathbb{P}(X > x) = 0 \quad \text{as} \quad x \to \infty, \tag{5.6}$$

for all $\lambda > 0$. For general stable random variables, we have the following proposition, which is presented without proof.

Proposition 5.4.
Let $X \sim S(\alpha, \beta, \gamma, \delta)$ with $\alpha \in (0, 2)$. Then

$$\lim_{x\to\infty} x^\alpha \mathbb{P}(X > x) = k_\alpha \frac{1+\beta}{2}\gamma^\alpha, \tag{5.7}$$

$$\lim_{x\to\infty} x^\alpha \mathbb{P}(X < -x) = k_\alpha \frac{1-\beta}{2}\gamma^\alpha, \tag{5.8}$$

where

$$k_\alpha = \left(\int_0^\infty t^{-\alpha}\sin(t)\mathrm{d}t\right)^{-1} = \begin{cases} \frac{1-\alpha}{\Gamma(2-\alpha)\cos(\pi\alpha/2)}, & \alpha \neq 1, \\ 2/\pi, & \alpha = 1. \end{cases} \tag{5.9}$$

The fact that the tail probabilities decay like a power law means that for $X \sim S(\alpha, \beta, \gamma, \delta)$ with $\alpha < 2$, we have $\mathrm{Var}[X] = \infty$. Consequently, the central limit theorem does not apply in this case. Since $\mathbb{E}[|X|^p] = \int_0^\infty \mathbb{P}(|X|^p > x)\mathrm{d}x$ for a general random variable X, we can use Proposition 5.4 to deduce the following result.

Theorem 5.5.
Let $X \sim S(\alpha, \beta, \gamma, \delta)$ be a stable random variable. Then

$$\mathbb{E}[|X|^p] < \infty \quad \Leftrightarrow \quad \begin{cases} p \in (-1, \infty), & \alpha = 2, \\ p \in (-\infty, \alpha), & \alpha \in (0,1), |\beta| = 1, \text{ and } 0 \notin \mathrm{supp}(X)^\circ, \\ p \in (-1, \alpha), & \text{otherwise}, \end{cases} \tag{5.10}$$

where $\mathrm{supp}(X)^\circ$ denotes the interior of the support of X.

The important case $S(\alpha, 0, \gamma, 0)$ is often called a symmetric α-stable Lévy random variable in the literature, and is often abbreviated as a SαS random variable. Note that in this case, the Lévy prefix does not indicate that the random variable follows a Lévy distribution. SαS random variables will become the building blocks of the important class of stochastic processes called linear fractional stable motions. These will be introduced in the subsequent section.

5.2 Linear Fractional Stable Motions

Since the pioneering work by Mandelbrot and van Ness [22], the fractional Brownian motion (fBM) has become one of the most prominent Gaussian processes. For a filtered probability space $(\Omega, \mathcal{F}, (\mathcal{F}_t)_{t\in\mathbb{R}}, \mathbb{P})$ and $H \in (0, 1)$, a fBM of Hurst index H is a continuous centered Gaussian process $B^H = (B_t^H)_{t\in\mathbb{R}}$ such that $B_0 = 0$ almost surely and with covariance function

$$\mathbb{E}[B_t^H B_s^H] = \frac{1}{2}\big(|t|^{2H} + |s|^{2H} - |t-s|^{2H}\big), \quad t, s \in \mathbb{R}. \tag{5.11}$$

The fBM is almost surely $(H-\varepsilon)$-Hölder continuous on compact intervals for all $\varepsilon > 0$. Consequently, the Hurst index H controls the regularity of the process with $H = 1/2$ corresponding to a standard Brownian motion as evident by (5.11). Furthermore, the fBM is self-similar and has stationary increments. It is also not a semimartingale unless $H = 1/2$, i.e. the case of a standard Brownian motion. For more details on the fractional Brownian motion, we refer to [25].

The paths of a fBM with $H \in (0, 1/2)$ are referred to as being "rough", while paths of a fBM with $H \in (1/2, 1)$ are called non-rough. Examples of rough and non-rough paths are seen in Figure 5.2, which shows simulated fBM paths with $10,000$ points each. It is clear

that the fBM becomes less rough and more well-behaved as H increases. For details on how to simulate paths of a fBM, we refer to [13].

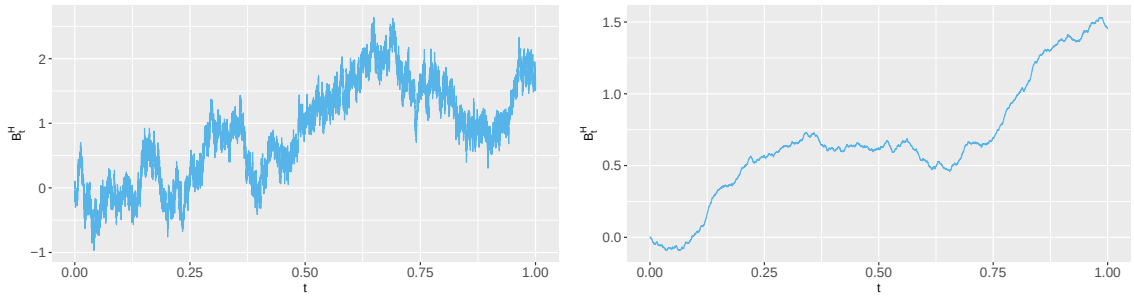

Figure 5.2: *Paths of fBMs of Hurst Indices* 0.25 *(left) and* 0.75 *(right).*

The Mandelbrot-Van Ness representation expresses a fBM in terms of stochastic integrals with respect to a two-sided Brownian motion W

$$B_t^H = C_H \left\{ \int_{-\infty}^{t} (t-s)^{H-1/2} \mathrm{d}W_s - \int_{-\infty}^{0} (-s)^{H-1/2} \mathrm{d}W_s \right\}, \tag{5.12}$$

where $C_H := \sqrt{\frac{2H\Gamma(3/2-H)}{\Gamma(H+1/2)\Gamma(2-2H)}}$. [22]

If we omit the Gaussianity assumption, the class of self-similar processes with stationary increments and a representation alike (5.12) becomes much larger. One such example is the linear fractional stable motion (LFSM).

Definition 5.6 (*Linear Fractional Stable Motion*)**.**
A linear fractional stable motion $Z = (Z_t)_{t\in\mathbb{R}}$ on the filtered probability space $(\Omega, \mathcal{F}, (\mathcal{F}_t)_{t\in\mathbb{R}}, \mathbb{P})$ is a process defined by

$$Z_t = \int_{\mathbb{R}} \left\{ (t-s)_+^{H-1/\alpha} - (-s)_+^{H-1/\alpha} \right\} \mathrm{d}L_s, \quad t \in \mathbb{R}, \tag{5.13}$$

where $x_+^p := \max\{x^p, 0\}$, $H \in (0,1)$, and $L = (L_t)_{t\in\mathbb{R}}$ is a symmetric α-stable Lévy motion with $\alpha \in (0,2]$ and scale parameter $\gamma > 0$.

That $L = (L_t)_{t\in\mathbb{R}}$ is a symmetric α-stable Lévy motion means that L has stationary and independent increments (whence Lévy) with distribution $L_t - L_s \sim S(\alpha, 0, |t-s|^{1/\alpha}, 0)$ for $t > s$.

In the case $\alpha = 2$, we have that Z is a fractional Brownian motion with Hurst index H, and consequently its paths are $(H-\varepsilon)$-Hölder continuous for all $\varepsilon > 0$. For $\alpha < 2$ and $H > 1/\alpha$, we have that the paths of Z are $(H - 1/\alpha - \varepsilon)$-Hölder continuous for all $\varepsilon > 0$. Otherwise, Z is measurable with unbounded paths on every compact interval. Furthermore, even when $H > 1/\alpha$ and $\alpha < 2$, the Hölder exponent of Z cannot exceed $1/2$. This is due to the fact that in this situation, we neccesarily have that $H < 1/2$ and $\alpha > 1$. In this case, we refer to Z as being "rough", and hence use the same nomenclature as for fBMs.

In the Gaussian case, i.e. $\alpha = 2$, we can formulate the Hölder continuity explicitly as follows; For every $T > 0$ and $\lambda \in (0, H)$, there exists a positive random variable $C_{\lambda,T}$, which depends on λ and T, such that

$$|Z_t - Z_s| \leqslant C_{\lambda,T} |t-s|^{\lambda}, \quad \forall t, s \in [0,T]. \tag{5.14}$$

Moreover, $C_{\lambda,T}$ has finite moments of all orders, see Theorem 1 in [4]. When $\alpha < 2$ and $H > 1/\alpha$, we can apply the Garsia-Rodemich-Rumsey inequality to choose $1 < \frac{1}{H-\lambda} < p < \alpha$ such that

$$|Z_t - Z_s| \leqslant C_{\lambda,T}|t-s|^{\lambda}, \quad \forall t, s \in [0,T], \tag{5.15}$$

where the positive random variable $C_{\lambda,T}$ is given by

$$C_{\lambda,T} = K\left(\int_0^T \int_0^T \frac{|Z_u - Z_v|}{|u-v|^{\zeta p+1}} \mathrm{d}u\mathrm{d}v\right)^{1/p}, \tag{5.16}$$

in which $\zeta = \lambda + 1/p$ with $\zeta \in (1/p, H)$, and K is a non-random positive constant, which depends on T, p, and ζ. If we let $q < \alpha$ and take some $p \leqslant q$, then by applying Minkowski's integral inequality and the self-similarity of X, we obtain that

$$\mathbb{E}[|C_{\lambda,T}|^q] \leqslant K\left(\int_0^T \int_0^T |u-v|^{p(H-\zeta)-1} \mathrm{d}u\mathrm{d}v\right)^{q/p} < \infty. \tag{5.17}$$

Consequently, $C_{\lambda,T}$ has moments of order $q < \alpha$.

5.2.1 Simulation of a Linear Fractional Stable Motion

This section is based on [31] and [20].

Suppose we wish to simulate the path of a LFSM Z on the interval $[0,T]$ for some $T > 0$. We will adopt the notation $\widetilde{Z}_{t_0}, \widetilde{Z}_{t_1}, \ldots, \widetilde{Z}_{t_N}$ for a simulated path of Z at the points $0 = t_0 < t_1 < \cdots < t_N = T$.

However, note that due to the self-similarity of Z, it is sufficient to simulate $(\tilde{Z}_0, \tilde{Z}_1, \ldots, \tilde{Z}_N)$, since we have that

$$(\widetilde{Z}_{t_0}, \widetilde{Z}_{t_1}, \ldots, \widetilde{Z}_{t_N}) \overset{\mathcal{L}}{=} (T/N)^H (\tilde{Z}_0, \tilde{Z}_1, \ldots, \tilde{Z}_N), \tag{5.18}$$

Furthermore, the simulation procedure we will present is approximate in a sense that will be made precise later. In the Gaussian case $\alpha = 2$, exact simulation techniques for fBMs such as Cholesky decomposition or the circulant embedding method can be applied instead, see [13]. We use the circulant embedding method for fBMs, since this is computationally much faster with a complexity of $\mathcal{O}(N \log N)$, whereas performing a Cholesky decomposition of the covariance matrix has a complexity of $\mathcal{O}(N^3)$. We refer to [20] for a comparison of the two methods.

Firstly, we note that we can normalize a LFSM in the sense that

$$Z_t = C_{H,\alpha}^{-1} \int_{\mathbb{R}} \left\{(t-s)_+^{H-1/\alpha} - (-s)_+^{H-1/\alpha}\right\} \mathrm{d}L_s, \quad t \in \mathbb{R}, \tag{5.19}$$

where $C_{H,\alpha}$ is a normalizing constant depending on H and α such that $\|Z_1\|_\alpha = 1$, which is given by

$$C_{H,\alpha} \coloneqq \left(\int_{\mathbb{R}} |(1-s)_+^{H-1/\alpha} - (-s)_+^{H-1/\alpha}|^\alpha \mathrm{d}s\right)^{1/\alpha}. \tag{5.20}$$

Let $V_k \coloneqq Z_k - Z_{k-1}$, $k \in \mathbb{Z}$, be the first-order increments of Z. Then by (5.19), we have that

$$V_k = C_{H,\alpha}^{-1} \int_{\mathbb{R}} g(k-s) \mathrm{d}L_s = -C_{H,\alpha}^{-1} \int_{\mathbb{R}} g(s) \mathrm{d}L_{k-s}, \tag{5.21}$$

where $g(s) \coloneqq (s)_+^{H-1/\alpha} - (s-1)_+^{H-1/\alpha}$. The stationary sequence $(V_k)_{k\in\mathbb{Z}}$ is called linear fractional stable noise.

The idea behind the simulation scheme is to use Riemann-sums to approximate the stochastic integral in (5.21) to obtain an approximate simulation of the noise V, and then take cumulative sums to obtain an approximate simulation of Z.

Firstly, we introduce the parameters $m, M \in \mathbb{N}$ and set

$$V_k^{m,M} := C_{H,\alpha}^{-1}(m,M) \sum_{j=1}^{mM} \Big((j/m)_+^{H-1/\alpha} - (j/m-1)_+^{H-1/\alpha} \Big) X_{mk-j}^{(m)}, \tag{5.22}$$

where $X_j^{(m)}$, $j \in \mathbb{Z}$, are independent random variables with the same SαS distribution $S(\alpha, 0, m^{-1/\alpha}, 0)$. The normalization constant $C_{H,\alpha}(m,M)$ is such that $\|V_1^{m,M}\|_\alpha = 1$ and is given by

$$C_{H,\alpha}(m,M) := m^{-1} \left(\sum_{j=1}^{mM} \left| (j/m)^{H-1/\alpha} - (j/m-1)_+^{H-1/\alpha} \right|^\alpha \right)^{1/\alpha}. \tag{5.23}$$

The parameters m and M control the precision of the integral computation, where m controls the mesh size, and M is a truncation parameter that determines the kernel function cut-off. We now consider the moving average process $W = (W_n)_{n\in\mathbb{N}}$ defined by

$$W_n := \sum_{j=1}^{mM} a_j^{H,m} X_{n-j}^{(1)}, \tag{5.24}$$

where $X_j^{(1)} \overset{\text{i.i.d.}}{\sim} S(\alpha, 0, 1, 0)$, $j \in \mathbb{Z}$, are i.i.d. standard SαS random variables, and the sequence $(a_j^{H,m})_{j\in\mathbb{N}}$ is given by

$$a_j^{H,m} := C_{H,\alpha}^{-1}(m,M) \Big((j/m)^{H-1/\alpha} - (j/m-1)_+^{H-1/\alpha} \Big) m^{-1/\alpha}, \quad j \in \mathbb{N}. \tag{5.25}$$

Since $\big\{X_j^{(m)},\ j \in \mathbb{Z}\big\} \overset{d}{=} \big\{m^{-1/\alpha} X_j^{(1)},\ j \in \mathbb{Z}\big\}$, we combine this in conjunction with (5.22) and (5.25) to deduce

$$\Big\{ V_k^{m,M},\ k = 1, \ldots, N \Big\} \overset{\mathcal{L}}{=} \{W_{mk},\ k = 1, \ldots, N\}, \tag{5.26}$$

where N is the number of generated points from the LFSM. Hence, our focus will be on computing the moving average W_n for $n = 1, \ldots, mN$. For large values of m and M, the moving average approximates V_k well in the sense that

$$(W_m, W_{2m}, \ldots, W_{Nm}) \xrightarrow[m\to\infty,\, M\to\infty]{\mathcal{L}} (V_1, V_2, \ldots, V_N). \tag{5.27}$$

In order to compute the moving average, we define the following two $m(M+N)$-periodic sequences by

$$\widetilde{X}_j^{(1)} := X_j^{(1)}, \quad j = 1, \ldots, m(M+N), \tag{5.28}$$

$$\widetilde{a}_j^{H,m} := \begin{cases} a_j^{H,m}, & j = 1, \ldots, mM, \\ 0, & j = mM+1, \ldots, m(M+N), \end{cases} \tag{5.29}$$

where the two sequences are extended to $\mathbb{Z}$ by simply repeating the patterns in (5.28) and (5.29). By (5.24), we now have

$$\big\{W_n\big\}_{n=1}^{mN} \overset{\mathcal{L}}{=} \left\{ \sum_{j=1}^{m(M+N)} \widetilde{a}_j^{H,m} \widetilde{X}_{n-j}^{(1)} \right\}_{n=1}^{mN}. \tag{5.30}$$

Finally, the discrete convolution of the sequences $(\widetilde{a}_j^{H,m})_{j\in\mathbb{Z}}$ and $(\widetilde{X}_j^{(1)})_{j\in\mathbb{Z}}$ is computed using the circular convolution theorem. This states that the convolution of two sequences can be computed as the inverse discrete Fourier transform of the product of the discrete Fourier transforms of the two sequences. The computation of the Fourier transforms is done efficiently using the Fast Fourier transform (FFT). After computing the convolution, we may take cumulative sums to obtain the desired sample $(\widetilde{Z}_1, \widetilde{Z}_2, \ldots, \widetilde{Z}_N)$ and rescale if necessary.

In Figure 5.3, we have simulated 2 LFSM paths Z_t along with their driving Lévy motions L_t on the unit interval with parameters $N = 2^{11} - 600$, $m = 256$, and $M = 600$. The top row shows the rough case $H < 1/\alpha$ with $H = 0.2$ and $\alpha = 1.4$, while the bottom row displays the case $H > 1/\alpha$ with $H = 0.8$ and $\alpha = 1.4$. In the rough case, the paths of Z_t are unbounded on every compact interval, and we see in the top row of Figure 5.3 how Z_t explodes at the jump times of L_t.

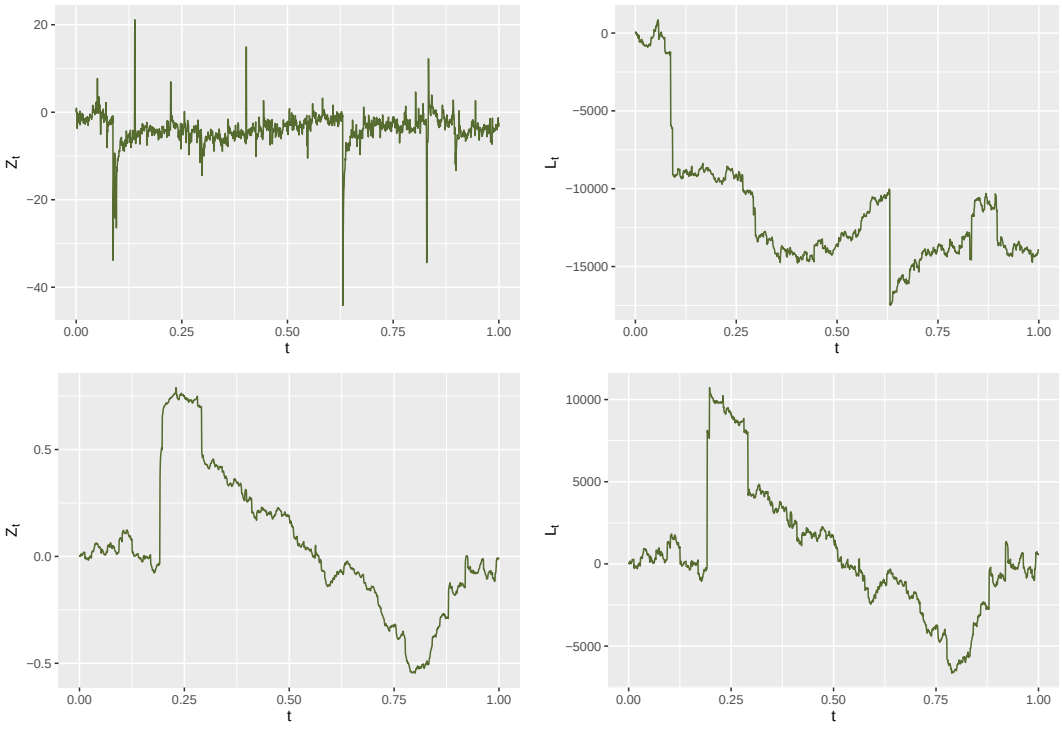

Figure 5.3: *Simulated LFSM Paths Z_t and Their Driving Lévy Motions L_t both in Rough Case $H < 1/\alpha$ (Top Row) and Non-Rough Case $H > 1/\alpha$ (Bottom Row).*

5.3 Stochastic Delay Differential Equations

This section is based on [29] and [21].

Stochastic differential equations (SDEs) play a vital role in stochastic calculus and financial mathematics. Recall that a general one-dimensional SDE takes the following form

$$X_t = X_0 + \int_0^t b(s, X_s)\,\mathrm{d}s + \sum_{j=1}^{m} \int_0^t \sigma^{(j)}(s, X_s)\,\mathrm{d}B_s^{(j)}, \quad t \geqslant 0, \tag{5.31}$$

where $b : [0,\infty) \times \mathbb{R} \to \mathbb{R}$ and $\sigma^{(j)} : [0,\infty) \times \mathbb{R} \to \mathbb{R}$ for $j = 1, \ldots, m$ are Borelian functions, and B is a m-dimensional standard Brownian motion. A solution to (5.31) is a triplet of the form $((\Omega, \mathcal{F}, (\mathcal{F}_t)_{t\geqslant 0}, \mathbb{P}), B, X)$ consisting of a filtered probability space satisfying the usual

conditions, a $\mathbb{R}^m$-valued Brownian motion B adapted to $(\mathcal{F}_t)_{t\geqslant 0}$, and the $(\mathcal{F}_t)_{t\geqslant 0}$-adapted continuous solution process X. In fact, we have that the solution process $X = (X_t)_{t\geqslant 0}$ is Markovian with respect to the filtration $(\mathcal{F}_t)_{t\geqslant 0}$.

However, we would like to be able to adjust the regularity of the solution process as well as introduce memory, or long-range dependence, into the solution process. In this section, we will introduce so-called Stochastic Delay Differential Equations (SDDEs), which can be seen as the generalization of classical SDEs to a non-Markovian framework. In particular, we will study SDDEs with additive noise, where the linear fractional stable motion will play the role as our noise process.

Definition 5.7 (*Stochastic Delay Differential Equation*)**.**
Let $(\Omega, \mathcal{F}, (\mathcal{F}_t)_{t\geqslant 0}, \mathbb{P})$ be a filtered probability space supporting a LFSM $Z = (Z_t)_{t\geqslant 0}$ with stability index $\alpha \in (0, 2]$. A stochastic delay differential equation with additive noise then takes the following form

$$\begin{aligned} X_t &= \psi(0) + \int_0^t \int_{[0,\tau]} b(X_{s-r})\, \eta(\mathrm{d}r)\mathrm{d}s + Z_t, \quad t \geqslant 0, \\ X_t &= \psi(t), \quad -\tau \leqslant t < 0, \end{aligned} \tag{5.32}$$

where $\tau > 0$, $\eta : \mathcal{B}([0,\tau]) \to \mathbb{R}$ is a finite, signed measure on $[0,\tau]$, $b : \mathbb{R} \to \mathbb{R}$ is measurable, and $\psi : [-\tau, 0] \to \mathbb{R}$ is a deterministic and continuous function that vanishes outside $[-\tau, 0]$.

For standard SDEs, we have existence and uniqueness, if the drift and diffusion components satisfy a global Lipschitz-condition in the spatial variable. For SDDEs of the form (5.32), we have the following result.

Theorem 5.8 (*Existence and Uniqueness*)**.**
Assume that $b : \mathbb{R} \to \mathbb{R}$ is Lipschitz-continuous and of linear growth, i.e.

$$\exists C > 0 : |b(x)| \leqslant C(1 + |x|). \tag{5.33}$$

Then the following holds

1. If $\alpha = 2$ or $\alpha < 2$ and $H > 1/\alpha$, then (5.32) admits a solution X with continuous paths satisfying
$$\mathbb{E}[|X_t|^p] < \infty, \quad \forall t > 0, \tag{5.34}$$
where $p < \alpha$ if $\alpha < 2$, and if $\alpha = 2$, then X has moments of all orders. Such a solution is unique, up to indistinguishability, within the class of continuous processes.

2. If $1 < \alpha < 2$ and $H < 1/\alpha$, then for each $T > 0$ there exists a measurable process X_t, $t \in [-\tau, T]$, satisfying (5.32) and which additionally satisfies
$$\mathbb{E}\bigg[\int_0^T \int_{[0,\tau]} |X_{s-r}|^p\, |\eta|(\mathrm{d}r)\mathrm{d}s \bigg] < \infty, \tag{5.35}$$
for $T > 0$ and $p \in [1, \alpha)$, and where $|\eta|$ is the total variation measure associated to η. Furthermore, we have
$$\sup_{-\tau \leqslant t \leqslant T} \mathbb{E}[|X_t|^p] < \infty, \tag{5.36}$$
and that the solution is unique, up to indistinguishability, within the class of measurable processes satisfying (5.35).

We now make the following remarks.

1. The solution process X inherits the path properties of Z. In particular, if $\alpha = 2$ and Z is a fBM, then X has $(H-\varepsilon)$-Hölder continuous paths for all $\varepsilon > 0$ on $[0,\infty)$. If $\alpha < 2$ and $H > 1/\alpha$, then X has $(H - 1/\alpha - \varepsilon)$-Hölder continuous paths for all $\varepsilon > 0$ on $[0,\infty)$.

2. If $\alpha \in (1,2)$, $H > 1/\alpha$, and b is of linear growth, then by combining a localization argument along with Grönwall's inequality and the self-similarity property of Z, one can show that for all $p \in [1,\alpha)$ and every $T > 0$, we have

$$\mathbb{E}\Big[\sup_{0\leqslant t\leqslant T}|X_t|^p\Big] \leqslant K_1\mathbb{E}\Big[\sup_{0\leqslant t\leqslant T}|Z_t|^p\Big]e^{K_2T^{p-1}} = K_1e^{K_2T^{p-1}}T^{pH}, \tag{5.37}$$

   for some positive constants K_1 and K_2. In the case of fBM $\alpha = 2$, the bound (5.37) still holds due to Theorem 1.1 in [26].

3. If the assumptions of Theorem 5.8 hold, then (5.37) above along with (5.14) and (5.16) give us the Hölder-condition

$$|X_t - X_s| \leqslant C_\lambda|t-s|^\lambda, \quad \forall t,s \in [0,T], \tag{5.38}$$

   where $T > 0$. If $\alpha = 2$ and $0 < \lambda < H$, then the positive random variable C_λ has finite moments of all orders p. If $\alpha < 2$, $H > 1/\alpha$, and $0 < \lambda < H - 1/\alpha$, then the positive random variable C_λ has finite moments of order $p < \alpha$.

5.3.1 Euler-Maruyama Scheme for SDDEs

As for SDEs, finding the solution of a given SDDE is generally a non-trivial task. Consequently, we may turn to numerical simulations of the solution process, and in particular, we will study the Euler-Maruyama scheme associated to (5.32). For this section, we will always assume that $\alpha \in (1,2]$, and that the assumptions of Theorem 5.8 are satisfied. Hence, a unique solution to (5.32) is guaranteed, which we denote by X. Additionally, we set

$$\mathcal{T}(s) \coloneqq \lfloor s/\Delta_{\tau,n}\rfloor\Delta_{\tau,n}, \quad s \geqslant 0, \;\; \Delta_{\tau,n} \coloneqq \tau/n, \tag{5.39}$$

for some $n \in \mathbb{N}$. We will adopt the notation X_t^n for a simulation at time t, and we define the Euler-Maruyama scheme associated to (5.32) as

$$X_t^n \coloneqq \begin{cases} \psi(0) + \displaystyle\int_0^t\int_{[0,\tau]} b\Big(X^n_{\mathcal{T}(s)-\mathcal{T}(r)}\Big)\,\eta(\mathrm{d}r)\mathrm{d}s + Z_t, & t \geqslant 0, \\ \psi(t), & -\tau \leqslant t < 0. \end{cases} \tag{5.40}$$

If we let $0 = t_0 < t_1 < \cdots < t_n = T$ be a partition of the interval $[0,T]$ for some $T > 0$, then for $t \in (t_{i-1}, t_i]$, $i = 1,2,\ldots,n$, we may observe that

$$X_t^n = X^n_{t_{i-1}} + (t-t_{i-1})\left(b(X^n_{t_{i-1}-\tau})\eta(\{\tau\}) + \sum_{j=1}^n b(X^n_{t_{i-1}-t_{j-1}})\eta([t_{j-1},t_j))\right) + Z_t - Z_{t_{i-1}}. \tag{5.41}$$

This implies that X^n is jointly measurable, and if the noise process Z is λ-Hölder continuous, then so is X^n. Furthermore, an application of Grönwall's inequality along with Theorem 5.8 gives us the following bound on the error

$$\mathbb{E}\Big[\sup_{t\leqslant T}|X_t - X_t^n|^p\Big] \leqslant C\Delta_{T,n}^{pH}, \tag{5.42}$$

for $p \geqslant 1$ if $\alpha = 2$ and for $p < \alpha$ if $\alpha < 2$, and C is some constant independent of n.

In order to implement the scheme in (5.41), we may pick an equidistant partition of $[0, T]$, i.e. $t_i = i\Delta_{T,n}$ for $i = 0, 1, \ldots, n$ and $\Delta_{T,n} \coloneqq T/n$. This simply corresponds to always picking the right endpoint of $(t_{i-1}, t_i]$ in (5.41). Furthermore, we may decompose the sum in (5.41) and obtain the following scheme

$$\begin{aligned} X_{t_i}^n =& X_{t_{i-1}}^n + \Delta_{T,n} b(X_{t_{i-1}-\tau}^n)\eta(\{\tau\}) + \Delta_{T,n} \sum_{j=1}^{i} b(X_{t_{i-1}-t_{j-1}}^n)\eta([t_{j-1}, t_j)) \\ &+ \Delta_{T,n} \sum_{j=i+1}^{n} b(\psi(t_{i-1} - t_{j-1}))\eta([t_{j-1}, t_j)) + Z_{t_i} - Z_{t_{i-1}}, \quad i = 1, 2, \ldots, n. \end{aligned} \tag{5.43}$$

Furthermore, we need to make some choices for b, η, and ψ. For the function b, we make a linear choice $b : x \mapsto ax$ for some $a \in \mathbb{R}$, which is certainly Lipschitz and of linear growth. For the measure η, we may pick

$$\eta(\mathrm{d}r) = -\lambda\delta_{\{0\}}(\mathrm{d}r) + \theta\delta_{\{\tau\}}(\mathrm{d}r), \quad \lambda, \theta \in \mathbb{R}, \tag{5.44}$$

where $\delta_{\{x\}}$ is the Dirac measure concentrated in the point x. Using this measure, the scheme (5.43) amounts to

$$X_{t_i}^n = X_{t_{i-1}}^n + \Delta_{T,n}\Big(b(X_{t_{i-1}-\tau}^n)\theta - b(\psi(0))\lambda\Big) + Z_{t_i} - Z_{t_{i-1}}, \quad i = 1, 2, \ldots, n. \tag{5.45}$$

Hence, this choice of measure puts all its weight at the endpoints 0 and τ.

Alternatively, we could pick a measure η, which is absolutely continuous with respect to the Lebesgue measure with the density

$$\eta(\mathrm{d}r) = e^{-\lambda r} r^\theta \mathrm{d}r, \tag{5.46}$$

where $\lambda \in \mathbb{R}$ and $\theta > -1$ are parameters. Using this measure, we obtain the scheme

$$\begin{aligned} X_{t_i}^n =& X_{t_{i-1}}^n + \Delta_{T,n} \sum_{j=1}^{i} b\Big(X_{t_{i-1}-t_{j-1}}^n\Big) \int_{[t_{j-1}, t_j]} e^{-\lambda r} r^\theta \, \mathrm{d}r \\ &+ \Delta_{T,n} \sum_{j=i+1}^{n} b(\psi(t_{i-1} - t_{j-1})) \int_{[t_{j-1}, t_j]} e^{-\lambda r} r^\theta \, \mathrm{d}r + Z_{t_i} - Z_{t_{i-1}}, \end{aligned} \tag{5.47}$$

for $i = 1, 2, \ldots, n$. By choosing n sufficiently large, we can make $|t_j - t_{j-1}| < \delta$ for any $\delta > 0$, and hence we may use the following Riemann-approximation for simulation

$$\int_{[t_{j-1}, t_j]} e^{-\lambda r} r^\theta \, \mathrm{d}r \approx (t_j - t_{j-1}) e^{-\lambda t_j} t_j^\theta, \quad j = 1, 2, \ldots, n. \tag{5.48}$$

For the initial function ψ, we want some continuous function on the interval $[-\tau, 0]$ satisfying the initial condition $\psi(0) = \psi_0$. Initially, we may pick a truncated Gaussian function of the form

$$\psi(t) \coloneqq \psi_0 e^{-t^2/2\beta^2} \mathbb{1}_{[-\tau, 0]}(t), \quad \beta > 0. \tag{5.49}$$

Note, however, that while (5.49) is continuous on $[-\tau, 0]$ and satisfies $\psi(0) = \psi_0$, we don't have $\psi(-\tau) = 0$.

If we want to ensure $\psi(-\tau) = 0$ and $\psi(0) = \psi_0$, we may use various interpolation techniques to obtain the function ψ. If we use a cubic Hermite spline on the interval $[-\tau, 0]$ with the specified initial conditions, we get

$$(\psi \circ u)(t) \coloneqq \tau\big(u(t)^3 - 2u(t)^2 + u(t)\big)m_\tau + \psi_0\big(-2u(t)^3 + 3u(t)^2\big) + \tau\big(u(t)^3 - u(t)^2\big)m_0,$$

where m_τ and m_0 are the desired slopes $\psi'(-\tau) = m_\tau$ and $\psi'(0) = m_0$, and $u(t) \coloneqq \frac{t+\tau}{\tau}$ is an affine function mapping $[-\tau, 0]$ bijectively to $[0, 1]$. If we pick $m_\tau = m_0 = 0$, we get a cubic spline of the simple form

$$\psi(t) = \psi_0 \left\{ -2\left(\frac{t+\tau}{\tau}\right)^3 + 3\left(\frac{t+\tau}{\tau}\right)^2 \right\}. \tag{5.50}$$

Finally, we may simply pick the first-degree linear interpolant through the points $(-\tau, 0)$ and $(0, \psi_0)$, i.e.

$$\psi(t) = \frac{\psi_0}{\tau} t + \psi_0. \tag{5.51}$$

Example 5.9.
We now consider a SDDE of the following Ornstein-Uhlenbeck type

$$\mathrm{d}X_t = X_{t-\tau}\mathrm{d}t + \gamma \mathrm{d}B_t^H, \quad t > 0, \tag{5.52}$$
$$X_t = \psi(t), \quad t \in [-\tau, 0], \tag{5.53}$$

where $\gamma \in \mathbb{R}$, $B^H = (B_t^H)_{t \geqslant 0}$ is a fBM of Hurst index $H \in (0, 1)$, and ψ is a continuous function on $[-\tau, 0]$. In this case, we have $\eta = \delta_{\{\tau\}}$ and $b(x) = x$, which is certainly Lipschitz-continuous and of linear growth, and hence we have a unique (up to indistinguishability) and continuous solution process X.

If we set $\phi_1(t) \coloneqq \psi(t)$, then for $t \in [0, \tau]$ we have that $t - \tau \in [-\tau, 0]$, and the SDDE (5.52) becomes the SDE

$$\mathrm{d}X_t = \phi_1(t-\tau)\mathrm{d}t + \gamma \mathrm{d}B_t^H \tag{5.54}$$

Rewriting (5.54) in its integral form, we get that

$$\begin{aligned} X_t &= \phi_1(0) + \int_0^t \phi_1(s-\tau)\,\mathrm{d}s + \int_0^t \gamma\,\mathrm{d}B_s^H \\ &= \phi_1(0) + \int_0^t \phi_1(s-\tau)\,\mathrm{d}s + \gamma B_t^H \\ &=: \phi_2(t). \end{aligned}$$

For $t \in [\tau, 2\tau]$, we have $t - \tau \in [0, \tau]$ and thus on this interval, the SDDE becomes

$$\mathrm{d}X_t = \phi_2(t-\tau)\mathrm{d}t + \gamma \mathrm{d}B_t^H.$$

We may again rewrite this in its integral form

$$\begin{aligned} X_t &= \phi_2(\tau) + \int_\tau^t \phi_2(u-\tau)\,\mathrm{d}u + \int_\tau^t \gamma\,\mathrm{d}B_u^H \\ &= \phi_2(\tau) + \int_\tau^t \left[\phi_1(0) + \int_0^{u-\tau} \phi_1(s-\tau)\,\mathrm{d}s + \gamma B_{u-\tau}^H\right]\mathrm{d}u + \int_\tau^t \gamma\,\mathrm{d}B_u^H \\ &= \phi_2(\tau) + \phi_1(0)(t-\tau) + \int_t^\tau \int_0^{u-\tau} \phi_1(s-\tau)\,\mathrm{d}s\mathrm{d}u + \int_\tau^t \gamma B_{u-\tau}^H\,\mathrm{d}u + \gamma(B_t^H - B_\tau^H) \\ &=: \phi_3(t). \end{aligned}$$

We can repeat this procedure iteratively on the intervals $[(i-1)\tau, i\tau]$ for $i = 3, 4, \ldots$, and construct the solution recursively.

We see that the solution $\phi_n(t)$ for $t \in [(n-2)\tau, (n-1)\tau]$ satisfies the recurrence relation

$$\phi_n(t) = \begin{cases} \phi_{n-1}((n-2)\tau) + \int_{(n-2)\tau}^{t} \phi_{n-1}(s-\tau)\,\mathrm{d}s + \gamma\Big(B_t^H - B_{(n-2)\tau}^H\Big), & n \geqslant 2, \\ \phi_1(t), & n = 1. \end{cases} \tag{5.55}$$

If we take $\tau = 1$, $\gamma = 1$, and ψ to be the cubic spline in (5.50) with $\psi_0 = 1$, we may simulate the solution process X on $[0, 1]$. In Figure 5.4, we have a solution process driven by a rough fBM with $H = 0.25$. The exact solution X is computed according to (5.55) with the Euler approximations X_t^n superimposed in red for various step sizes $\Delta_{T,n}$.

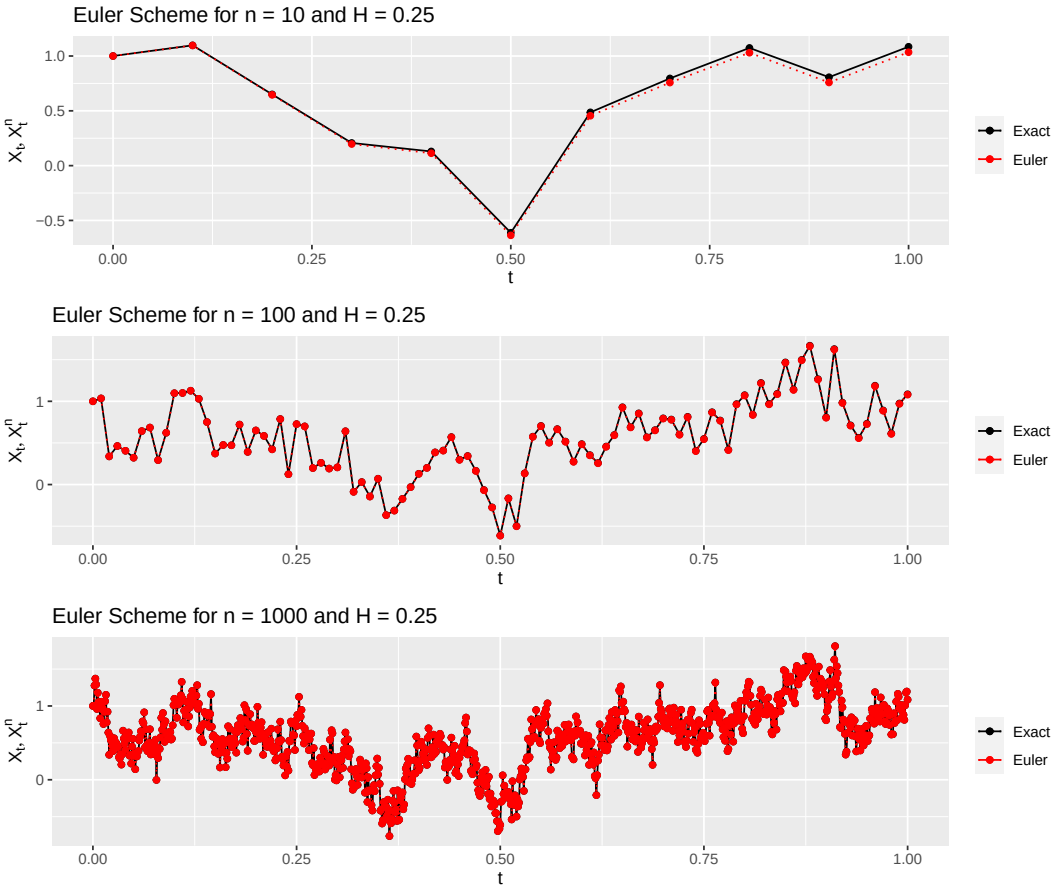

Figure 5.4: *Euler Approximations for Various Step Sizes $\Delta_{T,n}$ with $H = 0.25$.*

It is seen that already for $n \geqslant 100$, the true solution is approximated well by the Euler scheme. In Figure 5.5, the solution process X is driven by a fBM with $H = 0.75$, and we see that the Euler approximations X_t^n converge to the true solution faster than in the rough case. In particular, we see that already for $n = 100$, the exact solution and the Euler approximation start to become visually indistinguishable. For $n = 1000$, the Euler scheme is identically superimposed on the exact solution. The fact that the convergence is faster for the non-rough case than the rough case is proven in [29], which we refer to for details.

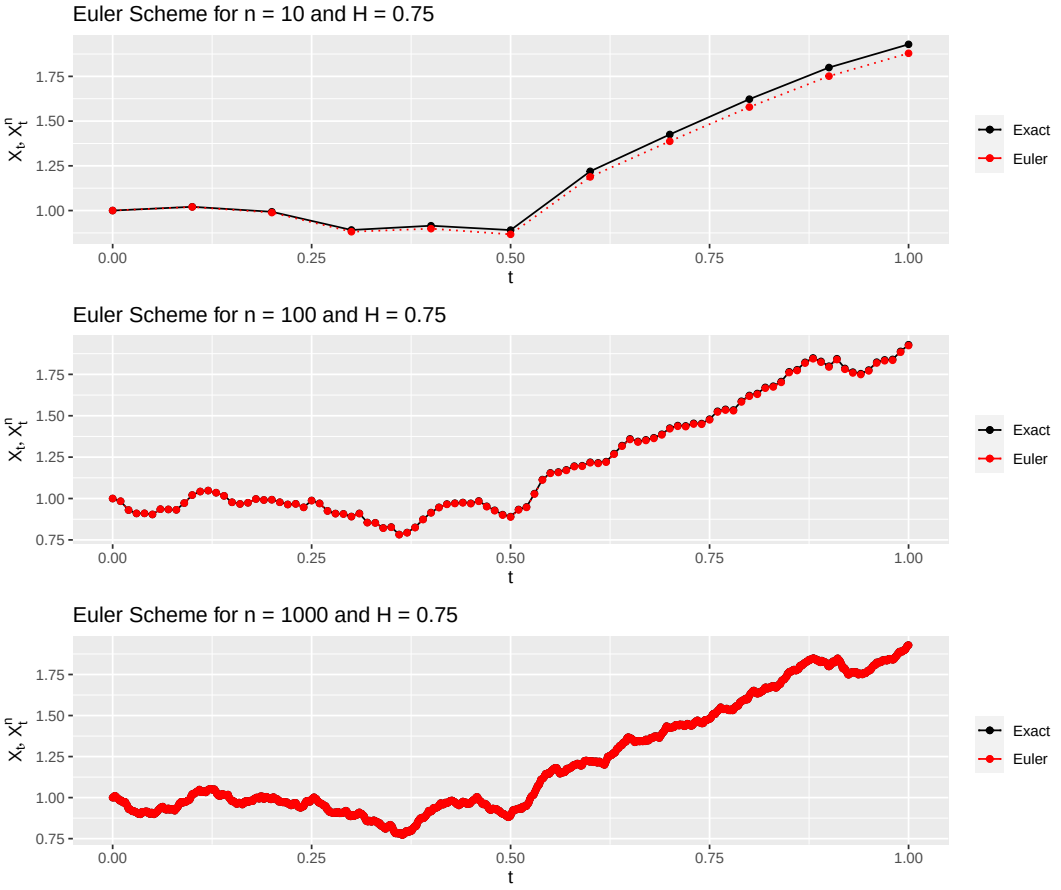

Figure 5.5: *Euler Approximations for Various Step Sizes* $\Delta_{T,n}$ *with* $H = 0.75$.

6 Simulation Study

In this chapter, we will conduct a simulation study in order to asses the power of the jump test introduced in Chapter 4. Firstly, we will asses the power of the test when applied to a number of standard Itô semimartingale processes both with and without jumps. Secondly, we will examine what happens when we apply the test to processes, which contain a rough volatility component, and thus are not semimartingales. In this way, we will examine whether the test is able to distinguish between rough volatility in the price process or actual jumps in the price process.

6.1 Choosing Parameters

We simulate the processes at different frequencies with an observation length of $t = 1$ trading day. Hence, we simulate the processes on the unit interval $[0, 1]$ in order to emulate 1 trading day of 6.5 hours. The highest frequency is $\Delta_n = 1$ second, which gives 23400 points in total, and the lowest frequency is $\Delta_n = 30$ seconds, which totals 780 points for a trading day. We simulate 1000 paths of the process for each frequency and choice of k, and all the price paths have a starting value of $S_0 = 100$. Please note that we use S_t throughout this chapter to denote log-prices of our model.

In accordance with [1], we set $p = 4$ in all our test. Hence, we have from (4.25) that asymptotically $\widehat{S}(4, k, \Delta_n)_t \to k$ on Ω_t^c. Furthermore, it is wise to choose k not too large, since the asymptotic variance increases with k. Additionally, for large values of k, we discard a lot of data, which leads to a decrease in the effective sample size used to compute the numerator $\widehat{B}(p, k\Delta_n)_t$. As in [1], we let $k \in \{2, 3, 4\}$ in our tests.

Finally, we have to choose the parameters C and ϖ used to compute $\widehat{A}(p, \Delta_n)_t$ in (4.31). Based on simulations, [1] argues that picking $\varpi = 0.47$ and letting C be between 3 and 5 times the average value of σ lead to good finite sample properties of the involved estimators. For a general financial time series, the spot volatility σ is a latent variable, which we cannot observe, but since we are simulating the processes, we will simply take C to be 4 times the average value of our simulated volatility component.

6.2 Itô Semimartingale Processes

The first model for prices is a standard geometric Brownian motion as previously studied in Section 3.2.1, i.e. we simulate the prices as

$$\mathrm{d}S_t = \mu \mathrm{d}t + \sigma \mathrm{d}B_t, \tag{6.1}$$

where B is a standard Brownian motion. For our simulations, we use $\mu = \sigma = 0.1$ as our drift and diffusion coefficients, respectively. When conducting a test on level $\alpha \in (0, 1)$, choosing the significance level α entails a probability of making mistakes, when choosing to

accept or reject the null hypothesis $\mathcal{H}_0$ of no jumps. The significance level is the probability of making a so-called Type 1 error, which means falsely rejecting the null hypothesis.

			Mean Value of $\widehat{S}(4,k,\Delta_n)$		Rejection Rate in Simulations	
Δ_n	n	k	Asymptotic	Simulations	10%	5%
1 sec	23 400	2	2	1.997	0.097	0.050
1 sec	23 400	3	3	3.000	0.094	0.044
1 sec	23 400	4	4	4.006	0.099	0.043
5 sec	4680	2	2	2.001	0.097	0.051
5 sec	4680	3	3	2.995	0.108	0.060
5 sec	4680	4	4	4.014	0.113	0.051
10 sec	2340	2	2	2.007	0.095	0.047
15 sec	1560	2	2	1.999	0.111	0.049
30 sec	780	2	2	2.001	0.101	0.053

Table 6.1: *Geometric Brownian Motion with* $\mu = \sigma = 0.1$.

In Table 6.1, we see that we make a Type 1 error as frequent as we expected. When testing on a 10% significance level, we reject the null hypothesis about 10% of the time, and equivalently our rejection rate is close to 5% for a significance level of 5%. The rejection rate at $\alpha = 0.1$ is slightly higher for $\Delta_n = 5$ seconds with $k = 4$ as well as $\Delta_n = 15$ seconds, which is expected, since the test is asymptotic. The mean values of the $\widehat{S}(4,k,\Delta_n)$ statistics are also extremely close to the asymptotic values of k.

The next process is the following stochastic volatility model as suggested in [11]

$$\mathrm{d}S_t = a\mathrm{d}t + \rho\sigma_t \mathrm{d}B_t + \sqrt{1-\rho^2}\sigma_t \mathrm{d}W_t, \tag{6.2}$$

where B and W are two independent Brownian motions and $\rho \in [-1,1]$. The logarithm of the spot volatility is modelled as an Ornstein-Uhlenbeck process, i.e. we have the following

$$\sigma_t = \exp(\beta_0 + \beta_1 X_t), \tag{6.3}$$
$$\mathrm{d}X_t = \theta X_t \mathrm{d}t + \mathrm{d}B_t, \tag{6.4}$$

where $\beta_0, \beta_1 \in \mathbb{R}$ and $\theta < 0$. The Ornstein-Uhlenbeck process X_t is simulated on the equidistant grid $0 = t_0 < t_1 < \cdots < t_n = T$ using the exact discretization

$$X_{t_{j+1}} = e^{\theta\Delta_n} X_{t_j} + \sqrt{-(2\theta)^{-1}(1-e^{2\theta\Delta_n})}\xi_{j+1}, \quad \xi_{j+1} \sim \mathcal{N}(0,1), \tag{6.5}$$

where $\Delta_n = T/n$. The initial value of the Ornstein-Uhlenbeck process is drawn randomly from its stationary Gaussian distribution $\mathcal{N}\big(0,(-2\theta)^{-1}\big)$. Hence, we get that X is automatically stationary. The parameter values we will use for our simulation study are

$$(a,\beta_0,\beta_1,\theta,\rho) = (0.03,-5/16,1/8,-1/40,-0.3). \tag{6.6}$$

With this choice of β_0, β_1, and θ, normalization of the volatility σ_t is ensured in the sense that

$$\mathbb{E}\left[\int_0^1 \sigma_s^2 \,\mathrm{d}s\right] = 1. \tag{6.7}$$

In Table 6.2, we report the testing results for simulations of the model (6.2) with the parameters (6.6).

			Mean Value of $\widehat{S}(4,k,\Delta_n)$		Rejection Rate in Simulations	
Δ_n	n	k	Asymptotic	Simulations	10%	5%
1 sec	23 400	2	2	1.999	0.099	0.048
1 sec	23 400	3	3	3.002	0.098	0.056
1 sec	23 400	4	4	3.992	0.086	0.040
5 sec	4680	2	2	2.004	0.098	0.051
5 sec	4680	3	3	3.003	0.095	0.050
5 sec	4680	4	4	3.992	0.102	0.047
10 sec	2340	2	2	1.997	0.111	0.053
15 sec	1560	2	2	1.998	0.104	0.046
30 sec	780	2	2	2.011	0.111	0.056

Table 6.2: *Stochastic Volatility Model in* (6.2) *with Parameters* (6.6).

Once again the test performs as expected with a rejection rate close to α in our simulations. Furthermore, we see that the rejection rates increase as Δ_n increases as was anticipated due to asymptotic specification of the test. However, the test generally performs very well and achieves a rejection rate close to α even with a mesh size of $\Delta_n = 30$ seconds.

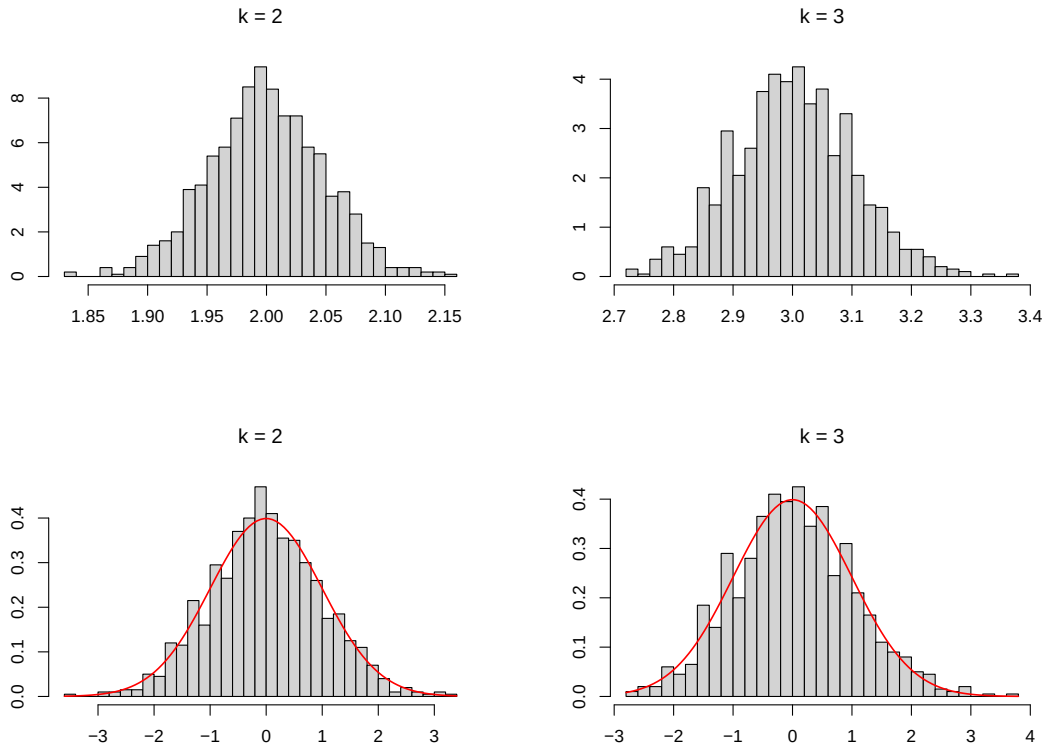

Figure 6.1: *Distribution of Non-Standardized (Top Row) and Standardized (Bottom Row) Test Statistics for* $\Delta_n = 1$ *second and* $k \in \{2, 3\}$.

In Figure 6.1, the distribution of the non-standardized test statistics $\widehat{S}(4,k,\Delta_n)_t$ from the tests performed in Table 6.2 at the $\Delta_n = 1$ second frequency for $k \in \{2,3\}$ are displayed in top row, and the standardized statistics in the bottom row. The non-standardized statistics are clearly centered around k as supported by the reported mean values in Table 6.2. From Theorem 4.7, we have that $(\widehat{V}^c_{n,t})^{-1/2}(\widehat{S}(p,k,\Delta_n)_t - k^{p/2-1}) \sim \mathcal{N}(0,1)$, which is also supported by the bottom row, where the Gaussianity of the standardized statistics clearly holds for both k. The standard normal density function is superimposed in red.

We now add jumps to the model in (6.2). Hence, we now consider the following model

$$S_t = S_0 + at + \rho \int_0^t \sigma_s \, \mathrm{d}B_s + \sqrt{1-\rho^2} \int_0^t \sigma_s \, \mathrm{d}W_s + \int_0^t Z_{N_s} \, \mathrm{d}N_s, \tag{6.8}$$

where N_t is a Poisson process with intensity $\lambda > 0$ and $Z_1, Z_2, \ldots, Z_{N_t}$ are i.i.d. random variables distributed as some common random variable Z. Hence, we now add a compound Poisson process to the stochastic volatility model, and we choose the jump distribution $Z \sim \mathcal{N}(0,1)$. In Figure 6.2, 3 paths of the process (6.8) with 23400 points each are displayed along with the accompanying compound Poisson processes and the volatility processes. The parameters are still (6.6) and the jump intensity is $\lambda = 1$, thus averaging 1 jump per day. However, we discard simulated paths that contain no jumps, and hence the actual number of jumps will be slightly higher than 1.

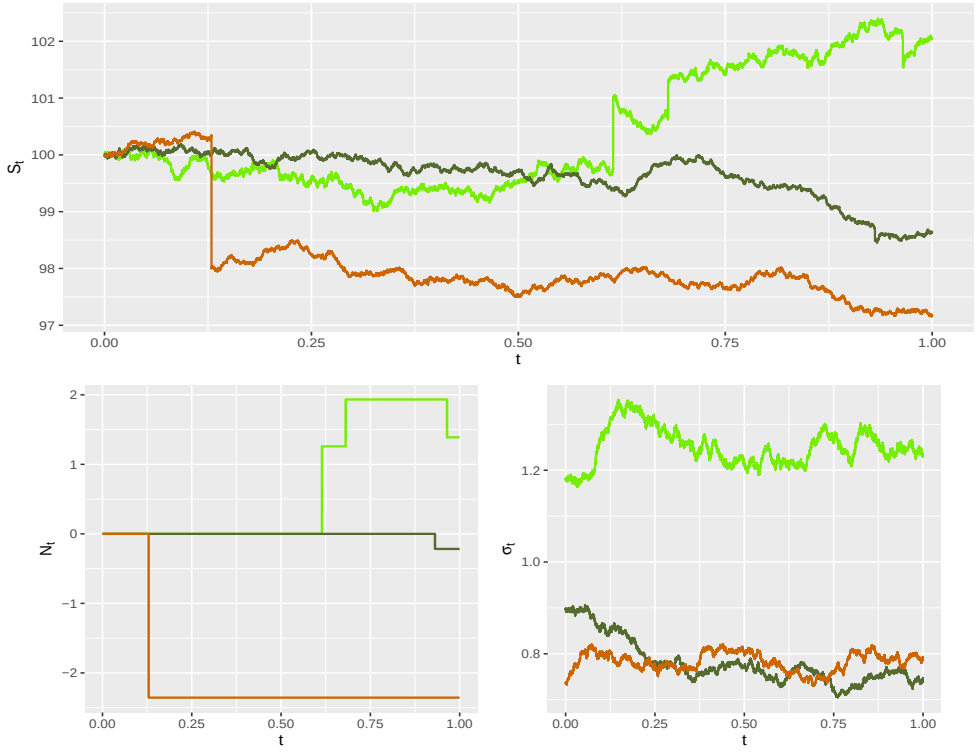

Figure 6.2: *Simulated Paths of* (6.8) *with Parameters* (6.6) *and* $\lambda = 1$.

In Table 6.3, we conduct the same testing methodology for the model (6.8) with jump intensities $\lambda \in \{1,3,6\}$ in order to asses the power of the test. Since the power function $\beta^c_{n,t}$ is conditional on the set Ω^j_t, we discard paths containing no jumps, and hence the actual intensities will be slightly higher than the reported λ.

	$\lambda = 1$		Mean Value of $\widehat{S}(4,k,\Delta_n)$		Rejection Rate in Simulations	
Δ_n	n	k	Asymptotic	Simulations	10%	5%
1 sec	23 400	2	1	1.038	0.988	0.987
1 sec	23 400	3	1	1.090	0.983	0.983
1 sec	23 400	4	1	1.176	0.975	0.969
5 sec	4680	2	1	1.085	0.950	0.946
5 sec	4680	3	1	1.167	0.955	0.945
5 sec	4680	4	1	1.200	0.965	0.962
10 sec	2340	2	1	1.091	0.953	0.942
15 sec	1560	2	1	1.115	0.925	0.915
30 sec	780	2	1	1.122	0.893	0.879
	$\lambda = 3$		Mean Value of $\widehat{S}(4,k,\Delta_n)$		Rejection Rate in Simulations	
Δ_n	n	k	Asymptotic	Simulations	10%	5%
1 sec	23 400	2	1	1.052	0.974	0.973
1 sec	23 400	3	1	1.110	0.974	0.972
1 sec	23 400	4	1	1.142	0.980	0.977
5 sec	4680	2	1	1.083	0.962	0.960
5 sec	4680	3	1	1.173	0.954	0.948
5 sec	4680	4	1	1.225	0.965	0.959
10 sec	2340	2	1	1.110	0.928	0.920
15 sec	1560	2	1	1.111	0.931	0.921
30 sec	780	2	1	1.126	0.892	0.877
	$\lambda = 6$		Mean Value of $\widehat{S}(4,k,\Delta_n)$		Rejection Rate in Simulations	
Δ_n	n	k	Asymptotic	Simulations	10%	5%
1 sec	23 400	2	1	1.057	0.974	0.974
1 sec	23 400	3	1	1.100	0.982	0.978
1 sec	23 400	4	1	1.155	0.972	0.970
5 sec	4680	2	1	1.082	0.948	0.945
5 sec	4680	3	1	1.166	0.956	0.954
5 sec	4680	4	1	1.283	0.948	0.945
10 sec	2340	2	1	1.097	0.936	0.923
15 sec	1560	2	1	1.101	0.925	0.915
30 sec	780	2	1	1.131	0.892	0.873

Table 6.3: *Stochastic Volatility Model with Jumps in* (6.8) *with Parameters* (6.6) *and Jump Frequencies* $\lambda \in \{1, 3, 6\}$.

From Theorem 4.5, we have that the random variables $\widehat{S}(p,k,\Delta_n)_t$ converge asymptotically to 1 on the set Ω_t^j, and the mean values of the simulations are all close to 1 for all frequencies Δ_n, k, and jump intensities λ. However, we seem to get the best results with $k = 2$. Furthermore, the power of the test, i.e. the probability that the test correctly

rejects the null hypothesis of no jumps conditional on Ω_t^j, is seen to be very good. At the high frequencies the test correctly rejects the null hypothesis for almost all paths. This is in accordance with Proposition 4.8, which states that the power function $\beta_{n,t}^c \to 1$ as $\Delta_n \to 0$. Expectedly, the power of the test gets progressively worse as the frequency gets lower, albeit it still performs relatively well and correctly rejects the null hypothesis in about 90% of the paths at $\alpha = 0.1$ at the 30 second frequency. Finally, we see that the power of the test seems unaffected by the jump frequency λ, since the rejection rate does not change significantly from $\lambda = 1$ to $\lambda = 6$.

6.3 Non-Semimartingales

In order to investigate whether the jump test can distinguish between rough volatility and jumps, we now replace the volatility process σ from the previous section with a "rough" process. In the previous section, we had $\sigma_t = \exp(\beta_0 + \beta_1 X_t)$, where X_t was an Ornstein-Uhlenbeck process. We now use the same stochastic volatility model in (6.2), but instead we use $\sigma_t = \exp(X_t)$, where the log-volatility process X_t is modelled as the Ornstein-Uhlenbeck type SDDE from Example 5.9 with delay $\tau = 1$ and $\gamma = 1$, i.e.

$$\mathrm{d}X_t = X_{t-1}\mathrm{d}t + \mathrm{d}B_t^H, \quad t \in (0,1], \tag{6.9}$$

$$X_t = \psi(t), \quad t \in [-1,0]. \tag{6.10}$$

Furthermore, we choose ψ to be the cubic spline in (5.50) with $\psi(0) = \log(0.1)$. In [10], Bolko et al. use a generalized method of moments approach to estimate the parameters in the rough fractional stochastic volatility (RFSV) model introduced by Gatheral et al. in [14] for the various stock indices in the Oxford-Man Institute's realized library. For the S&P 500 index, [10] obtain that $H = 0.043$, which we consequently use as the Hurst index for the fBM in (6.9).

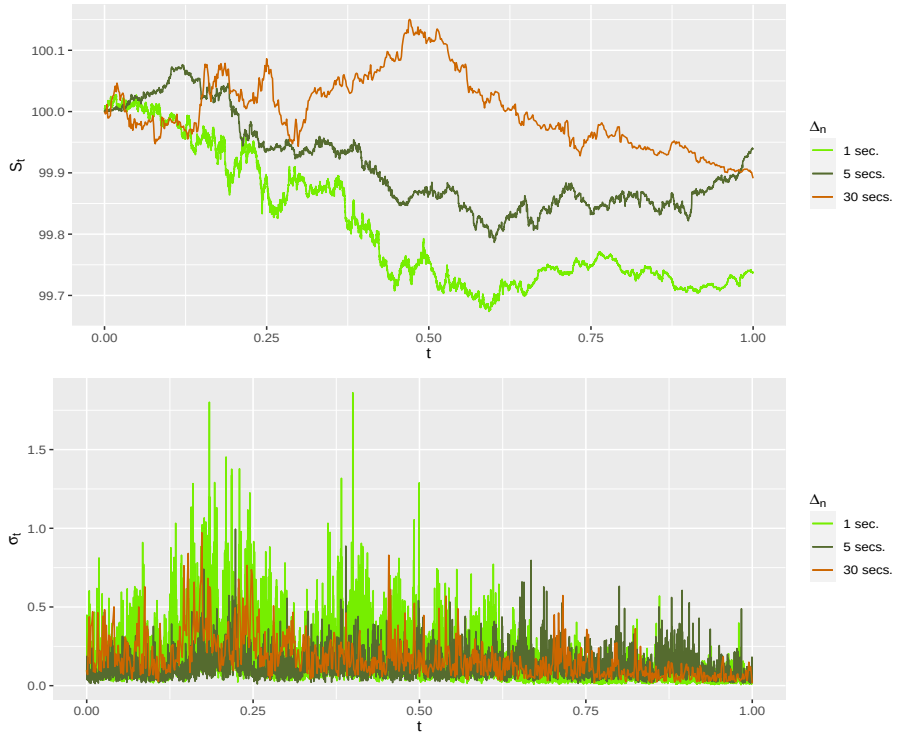

Figure 6.3: *Stochastic Volatility Paths at 1, 5, and 30 Second Frequencies (Top) with Rough Volatility Processes (Bottom) given by* (6.9).

In Figure 6.3, we have plotted 3 price paths of this model at different frequencies Δ_n along with their corresponding volatility processes. The volatility processes are extremely rough, and they share many of the qualitative features of observed financial volatility series. For example, they have persistent periods of high volatility that alternate with low volatility periods, i.e. they reproduce the stylized fact of volatility clustering. Consequently, the price paths are also more irregular with more erratic and jump-like behaviour.

			Mean Value of $\hat{S}(4,k,\Delta_n)$		Sample Variance	Rejection Rate in Simulations	
			Asymptotic	Simulations		10%	5%
Δ_n	n	k					
1 sec	23 400	2	2	1.456	0.065	0.982	0.979
1 sec	23 400	3	3	1.880	0.147	0.988	0.986
1 sec	23 400	4	4	2.334	0.215	0.992	0.989
5 sec	4680	2	2	1.428	0.107	0.891	0.857
5 sec	4680	3	3	1.864	0.344	0.921	0.893
5 sec	4680	4	4	2.252	0.543	0.918	0.874
10 sec	2340	2	2	1.412	0.131	0.821	0.759
15 sec	1560	2	2	1.413	0.172	0.738	0.654
30 sec	780	2	2	1.455	0.281	0.565	0.440

Table 6.4: *Stochastic Volatility with Rough Volatility Component with* $H = 0.043$.

In Table 6.4, we report the test results for the rough set-up, where we have also added a

column with the sample variance of the $\widehat{S}(4, k, \Delta_n)$ variables. At the 1 second frequency, we get very similar rejection rates to the rates in Table 6.3, since we reject the null hypothesis for almost all the paths. However, the $\widehat{S}(4, k, \Delta_n)$ variables do not approach 1 as they did in the case with jumps. As previously, their mean value increase with k, but here the increases are much bigger. The sample variances also increase with k, which is expected.

At the lower frequencies, the test becomes more indecisive, and the rejection rates drop significantly. At $\Delta_n = 30$ seconds, it rejects about half of the paths, and the mean value of the non-standardized $\widehat{S}$ statistics seems to be about halfway between 1 and 2.

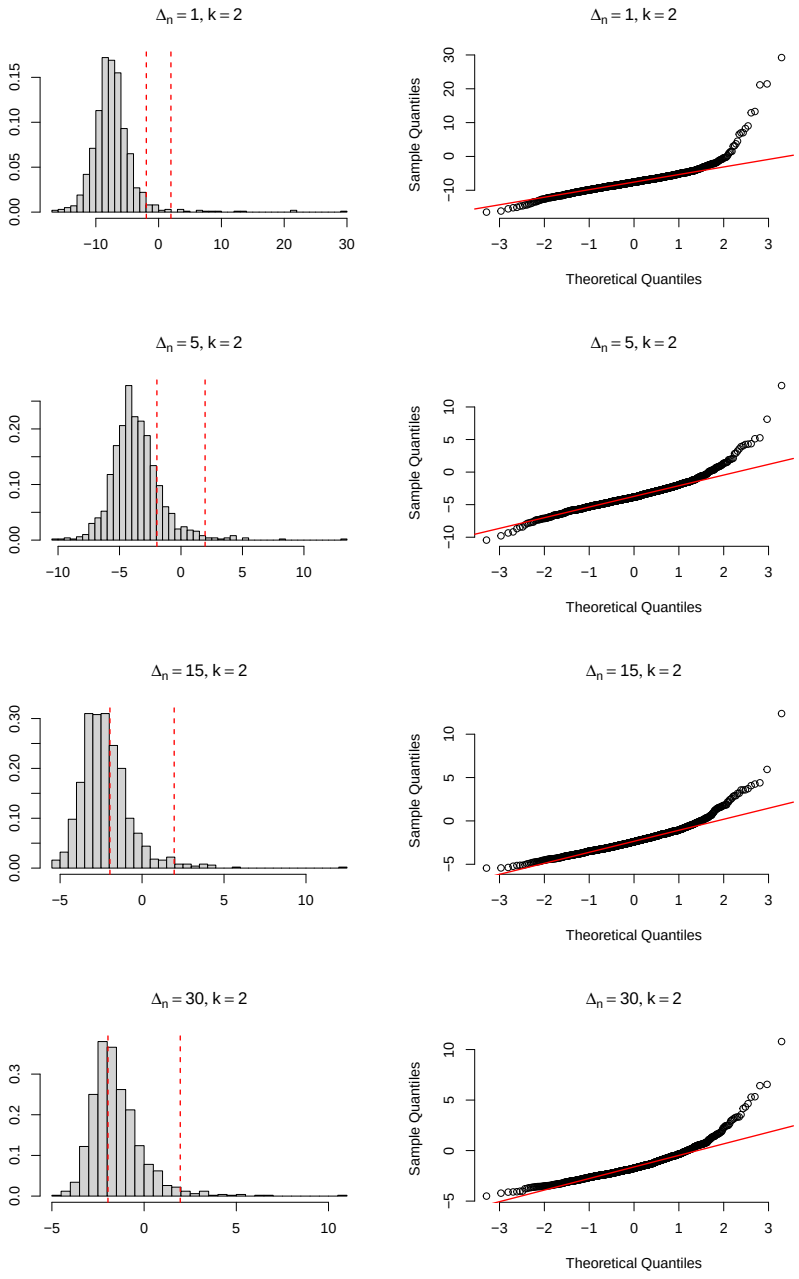

Figure 6.4: *Histograms and QQ-Plots for the Standardized Test Statistics with $k = 2$ at Different Frequencies.*

Figure 6.4 displays the distribution of the standardized test statistics in the rough case.

The vertical lines on the histograms are the standard normal quantiles $\Phi_{0.975} = 1.96$ and $\Phi_{0.025} = -1.96$, which determine the critical region when $\alpha = 0.05$. For $\Delta_n = 1$, almost all the test statistics fall within the critical region, and as Δ_n increases, less and less fall within the critical region. Although the distributions of the test statistics generally look Gaussian, as evident by the QQ-plots, they have fatter right-sided tails.

Finally, we may now turn to the RFSV model from [14], where the log-volatility is modelled as a fractional Ornstein-Uhlenbeck process

$$\mathrm{d}S_t = \mu_t \mathrm{d}t + \sigma_t \mathrm{d}W_t, \tag{6.11}$$

$$\sigma_t = \exp(X_t), \tag{6.12}$$

$$dX_t = -\kappa(X_t - m)\mathrm{d}t + \nu \mathrm{d}B_t^H, \quad X_0 = x_0, \tag{6.13}$$

where μ_t is a suitable drift term, W_t is a standard Brownian motion, $m \in \mathbb{R}$, $\kappa, \nu > 0$, and B^H is a fBM of Hurst index $H \in (0, 1/2)$. As for the standard Ornstein-Uhlenbeck process, there is an explicit form of the solution of (6.13), which is given by

$$X_t = m + e^{-\kappa t}\left(x_0 - m + \nu \int_0^t e^{\kappa s}\, \mathrm{d}B_s^H\right). \tag{6.14}$$

Furthermore, the variance of X_t is given by

$$\mathrm{Var}[X_t] = \frac{\nu^2}{2\kappa^{2H}}\Gamma(1 + 2H). \tag{6.15}$$

In [10], instead of estimating m directly, they instead estimate the auxiliary quantity

$$\xi = \exp\left(m + \frac{1}{2}\mathrm{Var}[X_t]\right). \tag{6.16}$$

They obtain the following estimates for the parameters in the fractional Ornstein-Uhlenbeck process calculated for the S&P 500.

κ	ν	ξ	H
0.001	1.610	0.019	0.043

Table 6.5: *GMM Estimated Parameters in* (6.13) *for S&P 500.*

Using the parameters in 6.5, we simulate the RFSV model with the price process being a driftless Itô process of the type

$$\mathrm{d}S_t = \sigma_t \mathrm{d}W_t, \tag{6.17}$$

where we assume $W \perp\!\!\!\perp B^H$.

In Figure 6.5, 3 realizations of the RFSV model with the parameters in Table 6.5 and $X_0 = \log(0.1)$ are depicted. The fractional Ornstein-Uhlenbeck process X_t, the volatility process $\sigma_t = \exp(X_t)$, and the price process are all displayed at different frequencies.

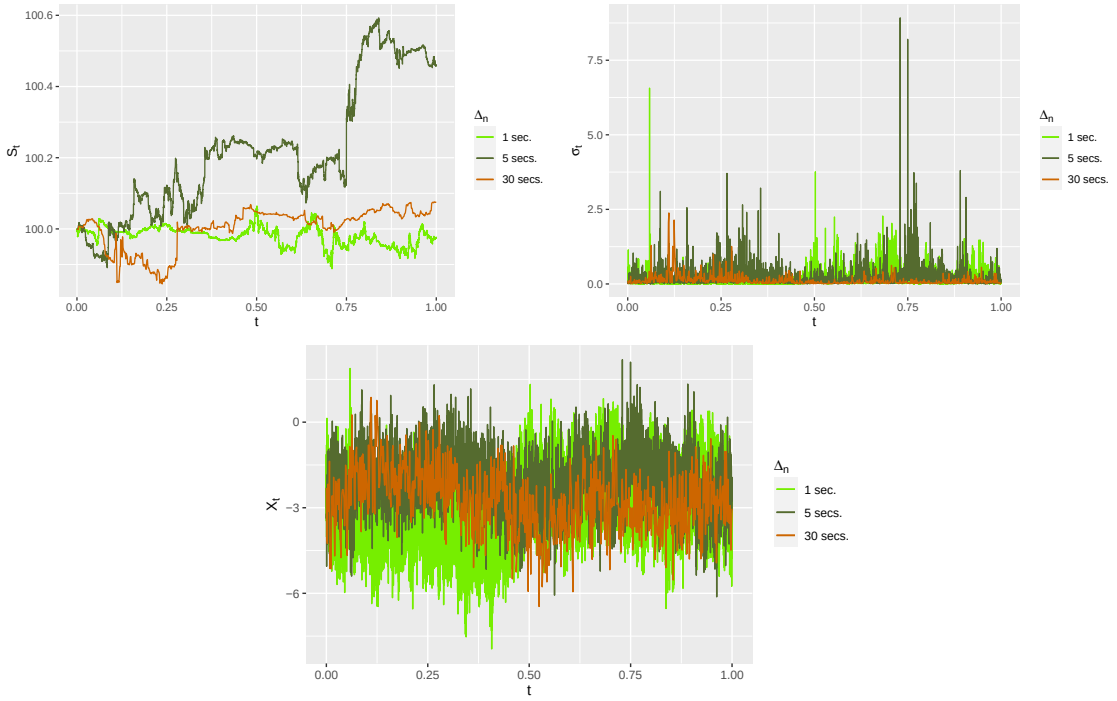

Figure 6.5: *Simulated Paths in RFSV Model with Parameters in Table 6.5.*

The small Hurst index $H = 0.043$ results in very rough paths of X_t with corresponding large spikes in the volatility process σ_t. The price process S_t is also more irregular than the previous model in Figure 6.3. The volatility processes share many of the qualitative features of the previous rough model, although the volatility spikes are considerably bigger. Hence, the price paths are also more erratic with big fluctuations that could easily be mistaken for jumps.

Consequently, the rejection rates summarized in Table 6.6 are close to 1. It is only for the lower frequencies that the rejection rates start to decline, although we still reject close to 90% of the paths at $\Delta_n = 15$ seconds for $\alpha = 0.1$. At the lowest frequency of $\Delta_n = 30$ seconds, the test becomes more indecisive, but we still reject far more paths than we did for the continuous non-rough processes in Table 6.1 or Table 6.2, where the rejection rates were close to α. The $\widehat{S}(4, k, \Delta_n)$ statistics also seem to be behave more like there are jumps present. Their mean values are closer to 1 for all values of k than they were in Table 6.4, and their mean values do not increase as significantly when k increases. The sample variances increase with k as expected. However, the sample variances are bigger at the $\Delta_n = 1$ frequency than they were in Table 6.4, but at the lower frequencies the sample variances are approximately the same for the 2 models.

			Mean Value of $\widehat{S}(4,k,\Delta_n)$		Sample Variance	Rejection Rate in Simulations	
Δ_n	n	k	Asymptotic	Simulations		10%	5%
1 sec	23 400	2	2	1.205	0.085	0.986	0.984
1 sec	23 400	3	3	1.381	0.275	0.992	0.987
1 sec	23 400	4	4	1.569	0.362	0.995	0.991
5 sec	4680	2	2	1.195	0.143	0.959	0.954
5 sec	4680	3	3	1.346	0.323	0.973	0.961
5 sec	4680	4	4	1.513	0.508	0.973	0.969
10 sec	2340	2	2	1.213	0.195	0.924	0.902
15 sec	1560	2	2	1.194	0.162	0.895	0.851
30 sec	780	2	2	1.198	0.212	0.800	0.704

Table 6.6: *RFSV Model with Parameters in Table 6.5.*

7 Conclusion

This Master's thesis investigates how jump tests perform, when they are tested against non-semimartingale price processes containing a rough volatility component. In particular, it investigates the jump test introduced by Aït-Sahalia and Jacod, which utilizes a ratio of power variations at different frequencies as its test statistic.

The jump test is asymptotic and hence only makes sense for high-frequency data. Consequently, the thesis contains a short digression into the characteristics of high-frequency financial data, and some of the pitfalls when dealing with this type of data. In the subsequent chapter, we introduce the integrated volatility, and how it can be estimated consistently using the realized covariation estimator. The realized covariation is a particular example of the so-called power variations, which are used to define our test statistic in the subsequent chapter.

The jump test by Aït-Sahalia and Jacod is then introduced, which uses a ratio of power variations to determine whether jumps are present in the observed path. The test statistic converges to 1, if jumps are present, and to another deterministic value if the path is continuous. We derive estimators for the asymptotic variance of the statistic, and we obtain that the standardized statistic follows a standard normal distribution. Furthermore, we have that the power function of the test converges to 1 as $\Delta_n \to 0$.

After introducing stochastic delay differential equations, we conduct a simulation study to investigate, how the test handles rough volatility. We initiate the analysis by considering the geometric Brownian motion and a stochastic volatility model. When tested on these two standard Itô semimartingale processes, the test performs largely as expected. The ratio of power variations $\widehat{S}(4, k, \Delta_n)$ converges as expected to k, and the rejection rates are approximately equal to the significance level α even at the lower frequencies. The distributions of $\widehat{S}(4, k, \Delta_n)$ are shown to be Gaussian, and the standardized statistics are shown to be standard normal. We then add a compound Poisson process to the stochastic volatility model in order to test for jumps. Conditional on the set Ω_t^j, the test statistics $\widehat{S}(4, k\Delta_n)$ converge to 1, and in our simulations they do indeed converge to 1. Furthermore, we have that the power function $\beta_{n,t}^c \to 1$ as $\Delta_n \to 0$, which is also the case for our simulations, where the rejection rates are very close to 1 for $\Delta_n = 1$ second. Additionally, the rejection rates seem to be invariant to the jump intensity λ.

If we instead take the log-volatility to be a stochastic delay differential equation with a rough fractional Brownian motion as noise term, the test seems to become more indecisive. At the high frequency of $\Delta_n = 1$ second, the rejection rates are very close to 1 as in the jump case. However, at the low frequency $\Delta_n = 30$ seconds, we have rejection rates of 56.5% and 44% at the significance levels $\alpha = 0.1$ and $\alpha = 0.05$, respectively. Whence the test is largely indecisive about whether jumps are present or not in the process at the 30 second frequency.

For this model, the statistics $\widehat{S}(4, k, \Delta_n)$ neither approach 1 nor k. However, they still seem to converge to a deterministic value for the different k, e.g. $\widehat{S}(4, 2, \Delta_n) \approx 1.4$ for all of

the different frequencies considered. Additionally, their distribution is still close to Gaussian, albeit with fatter right-sided tails. This indicates that the Gaussianity of the statistics still holds in the rough case, and that the ratio of power variations $\widehat{S}$ still converges to some deterministic value, which in the presence of rough volatility is neither 1 nor k.

Finally, we conduct an analysis of the RFSV model introduced in [14], and we use the parameters estimated for the S&P 500 in [10]. For this model, the price paths are more erratic, and the test largely behaves as in the jump case. The rejection rates are close 1 for the frequencies $\Delta_n = 1$ and $\Delta_n = 5$. Consequently, we conclude that the test is clearly unable to distinguish rough volatility from actual jumps, since all the rough price paths contain no jumps. This holds for both rough models, since the test breaks down in both cases.

For the RFSV model, the $\widehat{S}$ statistics still converge to a fixed value, which in this case is closer to 1 than the previous rough model. Hence, many of the distributional properties of the test seems to be intact in the rough setting, although the $\widehat{S}$ statistics converge to a new deterministic value, which depends on the k value used to compute it.

We leave further investigation of this question for future research.

Appendices

A Miscellaneous Definitions and Results

In this appendix, we state various definitions and technical results that are used throughout the project report, but stated here to ease the exposition.

A.1 Mixed Normal Distribution

Definition A.1 (*Mixed Normal Distribution*)**.**
Let X, M, Z be real-valued random variables defined on some probability space $(\Omega, \mathcal{F}, \mathbb{P})$, and let V be a non-negative random variable defined on the same probability space. Furthermore, let $Z \sim \mathcal{N}(0,1)$, and let M, V be independent of Z. We say X follows a mixed normal distribution with parameters M and V, written $X \sim MN(M, V)$, if

$$X = M + V^{1/2} Z. \tag{A.1}$$

A.2 Slutsky's Theorem

Theorem A.2 (*Slutsky's Theorem*)**.**
Let $(Y_n)_{n\in\mathbb{N}}$ and $(Z_n)_{n\in\mathbb{N}}$ be sequences of random variables defined on some probability space $(\Omega, \mathcal{F}, \mathbb{P})$, and assume that $Y_n \xrightarrow{\mathcal{L}} Y$ and $Z_n \xrightarrow{\mathcal{L}} c$ as $n \to \infty$, where $c \in \mathbb{R}$ is a constant. Then, as $n \to \infty$, we have the following

1. $Y_n + Z_n \xrightarrow{\mathcal{L}} Y + c$,
2. $Z_n Y_n \xrightarrow{\mathcal{L}} cY$,
3. $Y_n / Z_n \xrightarrow{\mathcal{L}} Y/c$ for $c \neq 0$.

A.3 Stable Convergence in Law

This section is based on [2] and [16].

Before introducing the notion of stable convergence in law, we firstly define what a Polish space is, and then what is understood by convergence in law.

Definition A.3 (*Completely Metrizable Space, Polish Space*)**.**
Let $(E, \mathcal{T})$ be a topological space. Then $(E, \mathcal{T})$ is said to be completely metrizable if there exists a metric $d : E^2 \to [0, \infty)$, which induces the topology $\mathcal{T}$, and such that (E, d) is a complete metric space. Furthermore, $(E, \mathcal{T})$ is said to be Polish, if it is completely metrizable and separable. Correspondingly, (E, d) is called a Polish metric space.

Definition A.4 (*Convergence in Law*)**.**
Let $(\Omega, \mathcal{F}, \mathbb{P})$ be a probability space, (E, d) a Polish metric space with Borel σ-algebra $\mathcal{E}$, and let $((\Omega_n, \mathcal{F}_n, \mathbb{P}_n))_{n\in\mathbb{N}}$ be a sequence of probability spaces. Then the sequence $Z_n : \Omega_n \to E$ of random variables is said to converge in law, if there exists a probability measure μ on $(E, \mathcal{E})$ such that

$$\int_{\Omega_n} f(Z_n(\omega))\,\mathrm{d}\mathbb{P}_n(\omega) \to \int_E f(x)\,\mathrm{d}\mu(x) \quad \text{as} \quad n \to \infty, \tag{A.2}$$

for every continuous and bounded function f on E.

Usually, one realizes the limit in (A.2) as a random variable Z with law μ. Specifically, we can take $X : E \to E$ as being the identity map $Z(x) = x$ on the probability space $(E, \mathcal{E}, \mu)$. Then (A.2) reads as

$$\mathbb{E}_n[f(Z_n)] \to \mathbb{E}[f(Z)] \quad \text{as} \quad n \to \infty, \tag{A.3}$$

for every continuous and bounded f on E, and we write $Z_n \xrightarrow{\mathcal{L}} Z$.

Furthermore, if each Z_n, $n \in \mathbb{N}$, is real-valued and absolutely continuous with distribution function F_n, then $Z_n \xrightarrow{\mathcal{L}} Z$ implies the pointwise convergence of the distribution functions $(F_n)_{n\in\mathbb{N}}$

$$F_n(x) \to F(x) \quad \text{as} \quad n \to \infty, \tag{A.4}$$

where F is the distribution function of Z, and x is a point of continuity for F.

For our purposes, convergence in law alone will not suffice, and we need a stronger form of convergence for random variables. Firstly, we need to define what is meant by an extension of our probability space.

Suppose we have a filtered probability space $(\Omega, \mathcal{F}, (\mathcal{F}_t)_{t\geqslant 0}, \mathbb{P})$, and let $(\Omega', \mathcal{F}')$ be another measurable space. Furthermore, let $\mathbb{Q}$ be a transition probability from $(\Omega, \mathcal{F})$ to $(\Omega', \mathcal{F}')$, i.e. $\mathbb{Q}(\omega, \cdot)$ is a probability measure on $(\Omega', \mathcal{F}')$ for $\omega \in \Omega$, and $\mathbb{Q}(\cdot, F')$ is a measurable function on $(\Omega, \mathcal{F})$ for $F' \in \mathcal{F}'$. We can then construct an extension in the following manner

$$\begin{aligned}
\widetilde{\Omega} &:= \Omega \times \Omega', \\
\widetilde{\mathcal{F}} &:= \mathcal{F} \otimes \mathcal{F}', \\
\widetilde{\mathbb{P}} &:= \mathbb{P}(\mathrm{d}\omega)\mathbb{Q}(\omega, \mathrm{d}\omega'),
\end{aligned}$$

where the last definition should be understood in terms of integrals, i.e. for $\widetilde{F} = F \times F' \in \mathcal{F} \otimes \mathcal{F}'$, we have

$$\int_{\widetilde{F}} g(\omega, \omega')\,\mathrm{d}\widetilde{\mathbb{P}}(\omega, \omega') = \int_F \int_{F'} g(\omega, \omega')\,\mathrm{d}\mathbb{Q}(\omega, \omega')\mathrm{d}\mathbb{P}(\omega), \tag{A.5}$$

for some $\widetilde{\mathcal{F}}$-measurable function g. Additionally, we may need to extend the filtration $(\mathcal{F}_t)_{t\geqslant 0}$. In order to this, we identify a set $A \subset \Omega$ with the set $A \times \Omega' \subset \widetilde{\Omega}$, and thus we can identify a σ-algebra $\mathcal{F}_t \subset \mathcal{F}$ with $\widetilde{\mathcal{F}}_t := \mathcal{F}_t \times \{\varnothing, \Omega'\} \subset \widetilde{\mathcal{F}}$ for $t \in [0, \infty)$. The filtered space $(\widetilde{\Omega}, \widetilde{\mathcal{F}}, (\widetilde{\mathcal{F}}_t)_{t\geqslant 0}, \widetilde{\mathbb{P}})$ is then called a filtered extension of $(\Omega, \mathcal{F}, (\mathcal{F}_t)_{t\geqslant 0}, \mathbb{P})$.

A filtered extension is called *very good* if the mapping

$$\omega \mapsto \int_{\Omega'} \mathbb{1}_A(\omega, \omega')\,\mathrm{d}\mathbb{Q}(\omega, \omega') \tag{A.6}$$

is $\mathcal{F}_t$-measurable for all ω and $A \in \widetilde{\mathcal{F}}_t$ for every $t \in [0, \infty)$. In particular, a very good filtered extension preserves the semimartingale property in the sense that any semimartingale on $(\Omega, \mathcal{F}, (\mathcal{F}_t)_{t\geqslant 0}, \mathbb{P})$ is also a semimartingale on $(\widetilde{\Omega}, \widetilde{\mathcal{F}}, (\widetilde{\mathcal{F}}_t)_{t\geqslant 0}, \widetilde{\mathbb{P}})$.

Definition A.5 (*Stable Convergence in Law*)**.**
Let $(\Omega, \mathcal{F}, \mathbb{P})$ be a probability space, (E, d) a Polish metric space with Borel σ-algebra $\mathcal{E}$, and let $(X_n)_{n\in\mathbb{N}}$ be a sequence E-valued random variables. Then we say $(X_n)_{n\in\mathbb{N}}$ converges stably in law, if there exists a probability measure μ on $(\Omega \times E, \mathcal{F} \otimes \mathcal{E})$ such that

$$\mathbb{E}[Y f(X_n)] = \int_{\Omega\times E} Y(\omega) f(x) d\mu(\omega, x) \tag{A.7}$$

for every bounded random variable Y and for every continuous and bounded function f on E.

Definition A.5 is an abstract definition, and similarly to Definition A.4, we may realize the limit as a random variable. Firstly, we may extend $(\Omega, \mathcal{F}, \mathbb{P})$ in the following manner

$$\widetilde{\Omega} := \Omega \times E,$$
$$\widetilde{\mathcal{F}} := \mathcal{F} \otimes \mathcal{E}.$$

We may endow $(\widetilde{\Omega}, \widetilde{\mathcal{F}})$ with the probability measure μ from Definition A.5. Furthermore, we may automatically extend any random variable Z_n on Ω to a random variable on $\widetilde{\Omega}$, with the same symbol, by setting $Z_n(\omega, x) = Z_n(\omega)$. Letting Z be an E-valued random variable defined on this extension, (A.7) is equivalent to saying

$$\mathbb{E}[Y f(Z_n)] \to \widetilde{\mathbb{E}}[Y f(Z)] \quad \text{as} \quad n \to \infty, \tag{A.8}$$

for every bounded random variable Y and every continuous and bounded function f on E. We then say that Z_n converges stably in law to Z, and we write $Z_n \xrightarrow{\mathcal{L}_s} Z$. Stable convergence obviously implies convergence in law, but it also implies much more than that. We have the following proposition from [27].

Proposition A.6.
Let Z_n, V_n, Z, Y, V be $\mathbb{R}^d$-valued, $\mathcal{F}$-measurable random variables and let $g : \mathbb{R}^d \to \mathbb{R}$ be a C^1 function.

1. If $Z_n \xrightarrow{\mathcal{L}_s} Z$ and $V_n \xrightarrow{\mathbb{P}} V$, then $(Z_n, V_n) \xrightarrow{\mathcal{L}_s} (Z, V)$.
2. Let $d = 1$ and $Z_n \xrightarrow{\mathcal{L}_s} Z \sim MN(0, V^2)$ with V being $\mathcal{F}$-measurable. Assume that $V_n \xrightarrow{\mathbb{P}} V$ and $V_n, V > 0$. Then $Z_n/V_n \xrightarrow{\mathcal{L}} \mathcal{N}(0, 1)$.
3. Let $\sqrt{n}(Z_n - Z) \xrightarrow{\mathcal{L}_s} Y$. Then $\sqrt{n}(g(Z_n) - g(Z)) \xrightarrow{\mathcal{L}_s} \nabla g(Z) Y$.

Bibliography

[1] Aït-Sahalia, Y. and Jacod, J. *Testing for Jumps in a Discretely Observed Process*. The Annals of Statistics, 37(1): 184-222 (2009).

[2] Aït-Sahalia, Y. and Jacod, J. *High-Frequency Financial Econometrics*, 1st edition. Princeton University Press (2014).

[3] Andersen, T. G., Bollerslev, T., Diebold, F.X., and Ebens, H. *The Distribution of Realized Stock Return Volatility*. Journal of Financial Economics, 61(1): 43-76 (2001).

[4] Azmoodeh, E., Scottinen, T., Viitasaari, L., and Yazigi, A. *Necessary and sufficient conditions for Hölder continuity of Gaussian processes*. Statistics and Probability Letters, 94: 230-235 (2014).

[5] Barndorff-Nielsen, O. E. and Shepard, N. *Estimating Quadratic Variation Using Realized Variance*. Journal of Applied Econometrics, 17(5): 457-477 (2002).

[6] Barndorff-Nielsen, O. E. and Shepard, N. *Power and Bipower Variation with Stochastic Volatility and Jumps*. Journal of Financial Econometrics, 2(1): 1-37 (2004).

[7] Barndorff-Nielsen, O. E., Graversen, S. E., Jacod, J., Podolskij, M., and Shepard, N. *A Central Limit Theorem for Realized Power and Bipower Variations of Continuous Semimartingales*. From Stochastic Calculus to Mathematical Finance, The Shiryaev Festschrift, 33-69 (2006).

[8] Barndorff-Nielsen, O. E. and Shepard, N. *Econometrics of Testing for Jumps in Financial Economics Using Bipower Variation*. Journal of Financial Econometrics, 4(1): 1-30 (2006).

[9] Black, F., and Scholes, M. *The Pricing of Options and Corporate Liabilities*. The Journal of Political Economy, 81(3): 637-654 (1973).

[10] Bolko, A. E., Christensen, K., Pakkanen, M. S., and Veliyev, B. *A GMM approach to estimate the roughness of stochastic volatility*. Journal of Econometrics, 235(1): 745-778 (2023).

[11] Christensen, K., Kinnebrock, S., and Podolskij, M. *Pre-averaging estimators of the ex-post covariance matrix in noisy diffusion models with non-synchronous data*. Journal of Econometrics, 159(1): 116-133 (2010).

[12] Cont, R. and Tankov, P. *Financial Modelling with Jump Processes*, 1st edition. Chapman and Hall (2003).

[13] Dieker, T. *Simulation of fractional Brownian motion*. University of Twente (2004).

[14] Gatheral, J., Jaisson, T., and Rosenbaum, M. *Volatility is Rough*. Quantitative Finance, 18(6): 933-949 (2018).

[15] Grigelionis, B. *On the representation of integer-valued random measures by means of stochastic integrals with respect to the Poisson measure*. Lithuanian Mathematics Journal, 11(1): 93-108 (1971).

[16] Hansen, E. *Sandsynlighedsregning på Målteoretisk Grundlag*, 4th edition. Department of Mathematical Sciences, University of Copenhagen (2004).

[17] Jacod, J. *Calcul stochastique et problémes de martingales*. Lecture Notes in Mathematics 714. Springer (1979).

[18] Jacod, J. *Asymptotic properties of realized power variations and related functionals of semimartingales*. Stochastic Processes and their Applications, 118(4): 517-559 (2008).

[19] Jacod, J. and Protter, P. *Discretization of Processes*, 1st edition. Stochastic Modelling and Applied Probability, Springer (2012).

[20] Jensen, C. B. *Advanced Topics with Applications: Rough Volatility*. Department of Mathematical Sciences, Aalborg University (2023).

[21] Le Gall, J. F. *Brownian Motion, Martingales, and Stochastic Calculus*, 1st edition. Springer (2016).

[22] Mandelbrot, B. B. and Van Ness, J. W. *Fractional Brownian Motions, Fractional Noises and Applications*. SIAM Review, 10(4): 422-437 (1968).

[23] Mazur, S. and Otryakhin, D. *Linear Fractional Stable Motion with the rlfsm R Package*. The R Journal, 12(1): 386-405 (2020).

[24] Nolan, J. P. *Univariate Stable Distributions: Models for Heavy Tailed Data*, 1st edition. Springer (2020).

[25] Nourdin, I. *Selected Aspects of Fractional Brownian Motion*, 1st edition. Springer (2012).

[26] Novikov, A. and Valkeila, E. *On some maximal inequalities for fractional Brownian motions*. Statistics & Probability Letters, 44(1): 47-54 (1999).

[27] Podolskij, M. and Vetter, M. *Understanding limit theorems for semimartingales: a short survey*. CREATES Research Paper (2009).

[28] Samorodnitsky, G. and Taqqu, M. S. *Stable non-Gaussian Random Processes: Stochastic Models with Infinite Variance*, 1st edition. Chapman & Hall (1994).

[29] Sauri, O. *Asymptotic Error Distribution of the Euler Scheme for Fractional Stochastic Delay Differential Equations with Additive Noise*. Department of Mathematical Sciences, Aalborg University (2024).

[30] State Street Global Advisors. *SPY: SPDR S&P 500 ETF Trust*. `https://www.ssga.com/us/en/intermediary/etfs/funds/spdr-sp-500-etf-trust-spy` (2024).

[31] Stoev, S. and Taqqu, M. S. *Simulation methods for linear fractional stable motion and FARIMA using the Fast Fourier Transform*. Fractals, 12(1) (2004).